Häussermann V, Gutstein CS, Bedington M, Cassis D, Olavarria C, Dale AC, Valenzuela-Toro AM, Perez-Alvarez MJ, Sepúlveda HH, McConnell KM, Horwitz FE, Försterra G. 2017. Largest baleen whale mass mortality during strong El Niño event is likely related to harmful toxic algal bloom. PeerJ 5:e3123 https://doi.org/10.7717/peerj.3123

Largest baleen whale mass mortality during strong El Niño event is likely related to harmful toxic algal bloom

Verena Häussermann[1, 2, 3], Carolina S Gutstein[4, 5, 6], Michael Beddington[7], David Cassis[8], Carlos Olavarria[9, 10], Andrew C. Dale[7], Ana M. Valenzuela-Toro[6, 11], Maria Jose Perez-Alvarez[9, 12], Hector H. Sepúlveda[13], Kaitlin M. McConnell[3], Fanny E. Horwitz[14], Günter Försterra[1, 3, 15]

[1]Facultad de Ciencias Naturales, Escuela de Ciencias del Mar, Pontificia Universidad Católica de Valparaíso, Valparaíso, Chile

[2]GeoBio-Center, Munich, Germany

[3]Huinay Scientific Field Station, Puerto Montt, Region de los Lagos, Chile

[4]Area de Patrimonio Natural, Consejo de Monumentos Nacionales, Santiago, Región Metropolitana, Chile

[5]Red Paleontológica U-Chile, Laboratorio de Ontogenia y Filogenia, Departamento de Biología, Facultad de Ciencias, Universidad de Chile, Santiago, Región Metropolitana, Chile

[6]Department of Paleobiology, National Museum of Natural History, Smithsonian Institution, Washington, District of Columbia, United States

[7]Scottish Association for Marine Science, Oban, Scotland, UK

[8]Centro de Investigación e Innovación para el Cambio Climático, Universidad Santo Tómas, Santiago, Chile

[9]Centro de Investigación Eutropia, Santiago, Región Metropolitana, Chile

[10]Centro de Estudios Avanzados en Zonas Aridas (CEAZA), La Serena, Chile

[11]Ecology and Evolutionary Biology, University of California, Santa Cruz, Santa Cruz, California, United States

[12]Instituto de Ecología y Biodiversidad (IEB), Facultad de Ciencias, Universidad de Chile, Santiago, Chile

PeerJ Preprints | https://doi.org/10.7287/peerj.preprints.2707v1 | CC BY 4.0 Open Access | rec: 6 Jan 2017, publ: 6 Jan 2017

[13]Departamento de Geofísica, Universidad de Concepción, Concepción, Chile

[14]Facultad de Ciencias Naturales y Oceanográficas, Universidad de Concepción, Concepción, Chile

[15]Department of Zoology, Ludwig-Maximilians-University, Munich, Germany

Corresponding Author: Carolina S. Gutstein, Vicuña Mackenna 84, Providencia, Región Metropolitana, Chile, e-mail address: sgcarolina@gmail.com

PeerJ Preprints | https://doi.org/10.7287/peerj.preprints.2707v1 | CC BY 4.0 Open Access | rec: 6 Jan 2017, publ: 6 Jan 2017

ABSTRACT

While large mass mortality events (MMEs) are well known for toothed whales, they have been rare in baleen whales due to their less gregarious behaviour. Although in most cases the cause of mortality has not been conclusively identified, some baleen whale mortality events have been linked to bio-oceanographic conditions, such as harmful algal blooms (HABs). In southern Chile, HABs can be triggered by the ocean-atmosphere phenomenon El Niño. The frequency of the strongest El Niño events is increasing due to climate change. In March 2015, by far the largest reported mass mortality of baleen whales took place in a gulf in southern Chile. Here we show that the synchronous death of at least 343, primarily sei, whales can be attributed to HABs during a building El Niño. Although considered an oceanic species, the sei whales died while feeding near to shore in previously unknown large aggregations. This provides evidence of new feeding grounds for the species. The combination of older and newer remains of whales in the same area indicate that MMEs have occurred more than once in recent years. Large HABs and reports of marine mammal MMEs along the north-east Pacific coast may indicate similar processes in both hemispheres. Increasing MMEs through HABs may become a serious concern in the conservation of endangered whale species.

PeerJ Preprints | https://doi.org/10.7287/peerj.preprints.2707v1 | CC BY 4.0 Open Access | rec: 6 Jan 2017, publ: 6 Jan 2017

INTRODUCTION

Although most populations of whales have been fully protected from industrial hunting for half a century, some were reduced to such low levels that recovery is still very slow (Baker & Clapham, 2004). Today, whales face additional threats, such as ship strikes, entanglement and by-catch, underwater noise, pollution and habitat loss (Clapham et al., 1999). Moreover, since ocean conditions directly influence quality and availability of the prey species of baleen whales, the effects of climate change will become a concern (Simmonds & Isaac, 2007).

Mass mortality events (MME) of marine mammals generally involve social species such as dolphins or sea lions, but are rare in baleen whales due to their less gregarious behaviour (Perrin et al., 2009a). When MMEs have occurred in baleen whales they have often extended over several months and large areas, involving mostly coastal whales (Table 1). In the Northeast Pacific, seven to eight times more gray whales (*Eschrichtius robustus*) washed ashore during the years 1999 and 2000 than is usual in such a time span. Of these, 106 died within a three-month period in Mexico (Gulland et al., 2005). In the course of 2012, 116 southern right whales (*Eubalaena australis*), mostly calves, washed ashore at their breeding ground in Valdés Peninsula, Argentina (Anonymous, 2015). During 2009, 46 humpback whales (*Megaptera novaeangliae*) stranded in Australia (Coughran et al., 2013) and 96 in Brazil during 2010, most of them calves and juveniles (Rowntree et al., 2013). Less frequent and much smaller in magnitude are sudden and locally restricted baleen whale mortalities. The largest of those involved 14 humpback whales which died around Cape Cod during five weeks in November 1987 (Geraci et al., 1989) (Table 1). The causes of most MMEs have not been conclusively identified (e.g. Anonymous, 2015; Coughran et al., 2013; Gulland et al., 2005); however, paralytic shellfish poisoning during harmful algal blooms (HABs) has been argued as one of the main likely causes (and this is also the case for other marine vertebrate mass mortalities; Geraci et al., 1989; Durbin et al., 2002; Doucette et al., 2006; Rowntree et al., 2013; Cook et al., 2015; D'Agostino et al., 2015; Wilson et al., 2015; Lefebre et al., 2016).

Harmful algal blooms have an extended record in southern Chile (particularly the genus *Alexandrium* with production of Paralytic Shellfish Toxins (PST). HABs have been of concern to fishermen and Patagonian communities since at least 1972, when the first mass intoxication was recorded (Suárez and Guzmán, 2005). Since then, the geographic region in which blooms have been detected has increased to over 1000 km north-south extent (Molinet et al. 2003). HABs have also become more frequent, becoming annual events with blooms normally occurring in large areas during the summer and fall (Guzmán et al., 2002). Due to the danger posed by these toxins, the Chilean government funds a monitoring program with over 200 sampling stations throughout the southern part of Chile, where phytoplankton and shellfish samples are obtained and later analysed for the presence of microalgae and their toxins (paralytic shellfish toxin PST, amnesic shellfish toxin AST, diarrheic shellfish toxin DST) (Suárez and Guzmán, 2005). Unfortunately, mainly due to the difficulty accessing many sites, these biotoxin data are only available for a limited coastal area of southern Chile.

PeerJ Preprints | https://doi.org/10.7287/peerj.preprints.2707v1 | CC BY 4.0 Open Access | rec: 6 Jan 2017, publ: 6 Jan 2017

Chilean Patagonia is a complex environment that hosts one of the largest and most extensive fjord regions, with a north-south extent of approximately 1,500 km (42ºS to 55ºS), covering an area of over 240,000 km^2 and with a coastline of more than 80,000 km, made up of numerous fjords, channels and islands. At the same time this is one of the least scientifically understood marine regions of the world (Försterra, 2009; Försterra et al., in press). Precipitation can locally exceed 6,000 mm per year and the tidal range can exceed 7 m. The prevailing strong westerly winds make its exposed shores amongst the most wave-impacted in the world (Försterra, 2009). These factors are responsible for the inaccessibility of a large part of this region. Chilean Patagonia is subdivided into the North, Central and South Patagonian Zone (for a summary of biogeography of the region see Häussermann and Försterra, 2005 and Försterra et al., in press). The remote area around Golfo de Penas and Taitao Peninsula (Fig. 1) is situated in the Central Patagonian Zone between 47 ºS and 48ºS. Except for two Chilean Navy lighthouses at Cabo Raper and San Pedro, the closest human settlements are more than 200 km away (Tortel, Puerto Aysén and Puerto Edén).

PeerJ Preprints | https://doi.org/10.7287/peerj.preprints.2707v1 | CC BY 4.0 Open Access | rec: 6 Jan 2017, publ: 6 Jan 2017

In general, Chilean Patagonia is influenced by the West Wind Drift, a largescale eastward (onshore) flow which diverges at the coast to form the northward Humboldt Current and the southward Cape Horn Current (Thiel et al., 2007). The fjordic nature of the coastline produces significant local complexity, with many inlets and dispersed freshwater sources. High productivity in these coastal waters (Fig. 2) is driven by the availability of both terrestrial nutrients, carried by large rivers originating at the Northern and Southern Patagonian Icefields, and marine nutrients (González et al., 2010; Torres et al., 2014). While this region experiences coastal winds that favor net coastal downwelling, intermittent and/or localized upwelling, in particular in summer and north of Taitao Peninsula (47°S), is expected to enhance the supply of marine nutrients to coastal waters, and the relative balance between upwelling and downwelling varies from year to year.

During a vessel-based scuba diving expedition, “Huinay Fiordos 24” (HF24), focused on benthic fauna between Golfo Tres Montes (northern Golfo de Penas, 46°30'W) and Puerto Eden (49°S), dead baleen whales and skeletal remains were discovered south of Golfo de Penas and at Golfo Tres Montes. Here we describe by far the largest ever recorded MME of baleen whales at one time and place. Our analyses focus on the location and cause of the mortality.

MATERIALS AND METHODS

Field surveys

PeerJ Preprints | https://doi.org/10.7287/peerj.preprints.2707v1 | CC BY 4.0 Open Access | rec: 6 Jan 2017, publ: 6 Jan 2017

The vessel-based HF24 scuba diving expedition, from April 15 to May 8, 2015, aimed to inventory the benthic fauna of the area between Golfo Tres Montes (northern Golfo de Penas, 46°30'W) and Puerto Edén (49°S). By chance, VH and her team discovered recently dead baleen whales and skeletal remains in and close to the entrance of the 14 km long Estero Slight and in the Canal Castillo situated 235 km to the south (Figs. 1, 3, Table 2). Georeferences and photographs of different views were taken, whales measured, and species and sex identified whenever possible. Between May 25 and 31, the Chilean Fisheries Service (SERNAPESCA), with the support of the Chilean Navy (Armada) and the Criminal Investigation Department of the Civil Police (PDI), organized a vessel-based trip to the location of the dead whales in Estero Slight to investigate possible anthropogenic reasons behind the mortality. During this trip, genetic samples for species identification were taken, one ear bone was extracted and stomach and intestine contents of two whales were tested for presence of PST and AST (Fiscalía de Aysén, 2015). During a subsequent aerial survey on-board a high wing airplane Cessna 206, between June 23 and 27, 2015, CSG, VH and FH surveyed the coasts along the shores of Golfo de Penas. This aerial survey covered the coastal area between the Jungfrauen Islands (48°S) and Seno Newman (46°39'S) from altitudes between 100m and 850m and at speeds between 100km/h and 200km/h (Figs. 1, 4, Table 2). Due to limited flying time (unstable weather conditions and the inability to refuel in the area) data collection was focused on counting whale carcasses, recording GPS positions and taking photographs. A GoPro camera filmed continuously until reaching Seno Newman. The researchers on the flight counted carcasses and marked their coordinates while an audio recorder captured the carcass number, position, orientation, photo number, photographer and geomorphology of the beach. Whale counts were repeated in all areas except Seno Newman due to adverse weather conditions. Since there are no landing opportunities in this remote and unpopulated area it was not possible to take samples or close-up photos, or to search for additional whale bones.

In addition to the whale carcasses and skeletons from the two surveys, some whale carcasses and skulls were reported between February and June 2015 by boat crews navigating the west coast of Taitao Peninsula and the coast between 49°15' and 51°S (Table 2). Between January 23 and March 1, 2016 (Expedition Huinay Fiordos 27) and between April 27 and May 30, 2016 (Expedition Huinay Fiordos 29), two additional vessel-based expeditions were carried out, each to Seno Escondido, Seno Newman and Estero Slight, with the aim of searching for new carcasses, taking samples for genetic and red tide analyses, and performing oceanographic transects. Data from those surveys are included here, but most of the analyses of the samples will be published in a separate paper.

Samples of marine invertebrates were collected under permit of Subsecretaria de Pesca y Acuicultura (R.EX. 1295 del 27.04.2016). Samples of cetacean carcasses were authorized by SERNAPESCA, Region de Aysen (Acta Numbers 2016-11-10 and 12).

Satellite image

A high resolution satellite image was taken of Seno Newman on August 13, 2015 using the Pleiades-1 Satellite. The 16-Bit ortho-rectified GeoTIFF Multispectral (R-G-B-NIR) and Panchromatic files have been analyzed to count whale carcasses and determine their geographic positions (Fig. 5). The whales identified in the satellite image were compared to the photos and GPS locations obtained during the overflight, and cross matched with reference to nearby geomorphological features.

Taxonomic analysis

Whales were identified in situ during the vessel-based expedition based on morphological characteristics. The species identification of the specimens from which tissue was sampled during the SERNAPESCA expedition to Estero Slight was confirmed genetically by MJP (Fiscalía de Aysen, 2015). A 675 bp fragment of mitochondrial DNA control region was amplified using the primers using the primers M13 Dlp1.5 5'-TGTAAAACGACAGCCAGTTCACCCAAAGCTGRARTTCTA-3' and 8G 5 ´GGAGTACTATGTCCTGTAACCA (Dalebout et al. 2005) and sequenced in both directions. Amplification reactions were performed in a total volume of 25 µl with 5 µl PCR buffer 10X, 2 µl MgCl2 50 mM, 1 µl of each primer, 2 µl dNTP 200 mM and 0.3 µl Taq DNA polymerase (Invitrogen Life Technologies) and 50 ng DNA. The PCR temperature profile was as follows: a preliminary denaturing period of 2 min at 94 ºC followed by 30 cycles of denaturation for 30 s at 94 ºC, primer annealing for 40 s at 56 ºC and polymerase extension for 40 s at 72 ºC. A final extension period for 10 min at 72 ºC was included.

Taphonomy

PeerJ Preprints | https://doi.org/10.7287/peerj.preprints.2707v1 | CC BY 4.0 Open Access | rec: 6 Jan 2017, publ: 6 Jan 2017

Analysis was carried out, following biostratinomic criteria, on different subsets of the whale remains recorded during the overflight and the vessel-based surveys. Characterization of the depositional state of the carcasses was based on a *post hoc* analysis of the assemblage, exclusively through photographs, classifying the carcasses into three taphonomic classes according to previous studies of biostratinomic processes in marine mammals (Pyenson et al., 2014, Liebig et al., 2003, 2007, Schäfer, 1972). The aspects considered were: anatomic position of the carcasses (ventral, dorsal or lateral side up; n=201), deposition site (rocky or sandy, n=295), and the disarticulation and degree of decay of the carcasses. These final two aspects were sorted into classes to estimate the sequence of disarticulation/decay addressing two aspects: time since death (n=245) and drift time/distance of the carcass (as a proxy to estimate the relative location of death, n=151).

To assess the time since death, three categories were defined, reflecting a straightforward order from the least decomposed to the most disarticulated carcass/skeleton. “Class 1” refers to carcasses in the lowest to relatively medium state of decomposition for these assemblages. Included in this category are complete carcasses with skin, complete carcasses without skin, and complete carcasses with partially exposed bones (see Fig. 6A). “Class 2” includes carcasses in a relatively greater state of decomposition but still maintaining their longitudinal axis, although some bones may be scattered (see Fig. 6B). Finally, “Class 3” refers to isolated skeletal remains with no soft tissue, such as skulls, dentaries or postcranial remains (see Fig. 6C). Thus, the sequence of “time since death” should reflect ranges from less than 3 months (Class 1), several months, but probably less than 6 months (Class 2), to a year or more (Class 3).

PeerJ Preprints | https://doi.org/10.7287/peerj.preprints.2707v1 | CC BY 4.0 Open Access | rec: 6 Jan 2017, publ: 6 Jan 2017

The analysis of the location of death, namely whether the carcasses are para-autochthonous or allochthonous, was addressed by evaluation of the time that the carcasses had remained floating in the water column and at the surface (see Schäfer, 1972). For this, we defined two classes, depending of the presence or absence of the skull, as a proxy for the time floating and the potential distance between the site of mortality and the observed site of deposition (Fig. 7) (Toots, 1965; Voorhies, 1969; Behrensmeyer 1973; Holz and Simoes, 2002; Liebig, 2003). Thus, “Class A” includes carcasses that preserve the skull and “Class B” includes those without a skull. For this analysis we excluded skeletons which were considered older than a year (minimum age, based on field observations of AVT from 2016 expedition to the site of the mortality).

A geomorphological analysis was made using photographs and Google Earth (Terrametrics, 2015). We classified the type of depositional locality (i.e. sand/pebble dominated beach or rocky outcrop) (Table 2) in order to assess the relationship between these aspects and the taphonomic categories mentioned above; for instance, whether carcasses that had been transported further and disarticulated (allochthonous) were more prevalent at high energy sites (i.e. rocky outcrops) and articulated (para-autochthonous) carcasses more prevalent in low energy environments (i.e. sandy beaches).

PeerJ Preprints | https://doi.org/10.7287/peerj.preprints.2707v1 | CC BY 4.0 Open Access | rec: 6 Jan 2017, publ: 6 Jan 2017

To compare the density of the death assemblages at Golfo de Penas with known extinct and extant death assemblages recorded in the literature, we measured linear dimensions of the geomorphological units (i.e. length and width of the beach), through the measure tool in Google Earth, using the highest resolution satellite images available, at sites where assemblages were found. In this manner, the geographic areas corresponding to the death assemblages were calculated and the density determined by dividing the number of specimens in each assemblage by its area.

Analysis of the petrotympanic complex (ear bone)

CSG studied the bones of the middle and inner ear of one whale, collected during the SERNAPESCA expedition. A volumetric computed tomography in the Morita tomograph (box of 60 mm, 500 cuts) was carried out. The images were visualized with Osirix Dicom viewer v 5.6 32-bit in search for fractures or micro-fractures, which would appear as black gaps in the bony tissue.

Analysis for toxins (PST/AST)

Bivalve tissue was sampled in Estero Slight on April 22 and on May 25, 2015 (2 samples in total), and in Estero Slight, Seno Newman and Seno Escondido between January 23 and March 1, and April 27 and May 30, 2016 (22 samples in total). The stomach content and intestine content of two whales from Estero Slight were sampled on May 25, 2015. On February, 2016, one sample of duodenum content was obtained from a freshly dead whale observed in Estero Slight. At the same period, one sample of surface-swimming *Munida* spp. was collected at 46º 29.730'S, 74°55.722'W. All samples were analyzed *in situ* for presence of PST using the protocol already described for the shellfish tissue and stomach content samples. Samples from 2015 were analyzed by DC, while the samples from 2016 were analysed by KMC. The tissue was homogenized using a blender and mixed in a 1:1 ratio with a field extraction fluid composed of 2.5 parts of rubbing alcohol (70%) to one part white vinegar. The mixture was then homogenized manually and filtered through a paper filter (paper filter #4). The extract obtained after filtration was then used to detect the presence of toxins through rapid field test kits from Scotia Rapid Testing for PST and AST. For this, 100 µl of the extract was placed in a test tube containing running buffer, mixed and then 100 µl of this mixture was placed in a lateral flow ELISA (enzyme-linked immunosorbent assay) test strip with antibodies specific for PST (saxitoxin and its derivative toxins) and AST (domoic acid). These tests were left to develop for 1 hour before the results were read.

PeerJ Preprints | https://doi.org/10.7287/peerj.preprints.2707v1 | CC BY 4.0 Open Access | rec: 6 Jan 2017, publ: 6 Jan 2017

Twenty-two phytoplankton samples were collected in Estero Slight, Seno Newman and Seno Escondido between January 23 and March 1, and April 27 and May 30, 2016, using a 20 µm mesh size plankton net in a vertical tow from 15 m depth. The phytoplankton present in these samples was concentrated using the net, and a 100 µl subsample was placed in a tube with 0.1 M acetic acid and mixed. 100 µl of this mixture were then added to a test tube containing running buffer and an aliquot of this mixture of the same volume was placed in a ELISA test strip for PST and left to develop for one hour before results were read.

These qualitative PST test strips are extremely sensitive due to the local toxin profile, which is high in GTX2/3, resulting in detection limits below 32 µg STX Eq/100 g of tissue. The detection limit for the AST tests was reduced to 2 ppm of domoic acid by modifying the standard sample preparation protocol by eliminating the dilution of the sample before mixing it with the buffer.

A graphical analysis of the geographic and temporal distribution of PSP events, presence of harmful microalgae and environmental variables in the affected region (43°S-51°S) from 2007 to July 2015 and from March 2016 was performed with the data obtained from the red tide monitoring program conducted by the SERNAPESCA (RS Galdames RS, personal communication, 2015), in which mytilid samples are analyzed at several stations throughout Chilean Patagonia approximately once a month by the “Laboratorios SEREMI Salud”, from Aysén and Magallanes regions at southern Chile.

Drift model

PeerJ Preprints | https://doi.org/10.7287/peerj.preprints.2707v1 | CC BY 4.0 Open Access | rec: 6 Jan 2017, publ: 6 Jan 2017

Floating objects are directly affected by surface currents, wind and waves. Wind both drives the Ekman drift of surface water (Ardhuin et al., 2009) and exerts a direct drag on the emerged surface of an object (Breivik et al., 2012). Stokes drift, the net forward transport due to non-closed particle trajectories resulting from passing waves, also contributes to the transport of floating objects. The drift of whale carcasses was simulated by parametrising the contribution of these components, based on objects of a similar size from search and rescue models (Breivik et al., 2012; Peltier et al., 2012). Due to the large uncertainty in carcass drift characteristics, parameters were varied stochastically within a wide range of possible values.

Use was made of existing current and wave products, the HYCOM daily 1/12 simulation (Wallcraft et al., 2009), and waves from ECMWF ERA-Interim reanalysis (Dee et al., 2011). Winds were taken from a custom downscaling of NCEP NFL boundary conditions using the WRF model (Skamarock et al., 2008) to a sub-4 km grid size. Drift scenarios were run by stepping forward in time from hypothetical sites and times of mortality. All of these sites were in shallow water, since carcasses resulting from mortality in deep water have a tendency to sink and not resurface (Smith et al., 2015). A horizontal diffusion coefficient of 10 m^2s^{-1} was included in drift tracks to represent unresolved physical processes. While the resolution of the current and wave datasets is inadequate to represent detailed coastline or seabed geometry, or the interior of the fjords, the drift model does clarify the expected distribution and spread of carcasses from localized sources.

Large scale wind stress

PeerJ Preprints | https://doi.org/10.7287/peerj.preprints.2707v1 | CC BY 4.0 Open Access | rec: 6 Jan 2017, publ: 6 Jan 2017

The large-scale tendency toward upwelling or downwelling provides a key driver of coastal ecosystems. This was assessed using ECMWF ERA-Interim reanalysis data (Dee et al., 2011). It is the alongshore component of wind stress that drives Ekman transport normal to the coast and consequent upwelling or downwelling. Since upwelling and downwelling are cumulative processes, a time-integrated wind stress was calculated (e.g. Pierce et al., 2006) from a base time of the vernal equinox (September 21). Stress was estimated from reanalysis winds at 10 m elevation according to Large and Pond (1981). The large scale change in coastal orientation was taken into account in extracting the alongshore wind component, although localized inlets, bays (including the Golfo de Penas) and islands were not considered.

RESULTS

Field surveys and toxicity tests

Of the total of dead whales observed in all expeditions and reports in 2015 (367), 35 recently dead whales and 12 skeletal remains were discovered during the HF24 expedition: 31 carcasses and 12 skeletal remains were found in and close to the entrance of the 14 km long Estero Slight and four carcasses in Canal Castillo, situated 235 km to the south, as well as many whale bones on different beaches (Fig. 3, Table 2). Three-hundred and five carcasses were mapped during the overflight between the Jungfrauen Islands (~48ºS) and Seno Newman (46º39'S). In addition to this total of 284 whale carcasses and 21 skeletons from the two surveys, 51 whale carcasses and 11 whale skulls were reported between February and June 2015 by boat crews navigating the west coast of Taitao Peninsula and the coast between 49°15' and 51°S (Table 2, Fig. 4).

PeerJ Preprints | https://doi.org/10.7287/peerj.preprints.2707v1 | CC BY 4.0 Open Access | rec: 6 Jan 2017, publ: 6 Jan 2017

On some photos what could have been carcasses of smaller animals (possibly dolphins and/or sea lions) were seen, but due the flying altitude, speed and weather conditions, the photo quality and resolution did not allow their conclusive identification as actual carcasses. In Estero Slight, one dead pinniped was found on the shore from the vessel. During the SERNAPESCA expedition one Otariidae skull was found and photographed in the same channel but the correspondence of the carcass and the skull could not be established.

The 28 whale carcasses that could be identified unambiguously to species level were all sei whales (*Balaenoptera borealis*); 15 of these identifications were confirmed genetically. Seven specimens could be identified as males and ten as females. One hundred and twenty-nine carcasses were identified as baleen whales of the Balaenopteridae family or rorquals. The 30 whales examined in detail in Estero Slight during the vessel-based expedition were between 6 m and 15 m long, hence included both juvenile and fully grown specimens.

None of the examined whales showed any evidence of disease or traumatic damage. The anatomic structures of the ear bone were in good condition showing no damage; the stapes were articulated in place, and the bony tissue showed no fractures (Fig. 8). The analysis of locally collected mytilids in April and May 2015 and of the stomach and intestine content of two whales in May 2015 showed presence of PST and AST.

PeerJ Preprints | https://doi.org/10.7287/peerj.preprints.2707v1 | CC BY 4.0 Open Access | rec: 6 Jan 2017, publ: 6 Jan 2017

In 2016, 16 fresh carcasses were observed during the HF27 and HF29 vessel-based expeditions to Golfo Tres Montes; five further were reported by boat crews navigating the southern part of Chilean Patagonia. None of the examined whales showed any evidence of disease or traumatic damage. Thirty-six rapid tests on PST were run using mussels (12 tests), *Munida* (2 tests), and phytoplankton (22 tests) in Seno Escondido, Seno Newman and Estero Slight. Most of the samples collected during the 2016 expeditions proved to be negative for the presence of PST, nevertheless, both expeditions detected the presence of PSP in the phytoplankton collected at the entrance of Seno Newman. A sample collected at the head of Seno Newman was negative for PST, indicating that the toxic phytoplankton was preferentially located at the mouth of this inlet and nearby areas of the Canal Chaicayán.

Biostratinomic analysis

Of the 367 dead whales observed in 2015, 305 carcasses were mapped between Seno Newman (46º39'S) and Jungfrauen Islands (~48ºS). Those carcasses could be grouped into five assemblages (Figs. 1, 9, Table 2), defined as a group of carcasses in close proximity. The assemblages were called Golfo de Penas, Jungfrauen Islands, Seno Escondido, Seno Newman and Estero Slight.

Some carcasses were floating (11), but most (284) were deposited ashore (Figs. 3 to 5). In general, they were tide-oriented (parallel to the coast line) and all of the classified carcasses from the overflight were lying on their back or side (ventral up, 44.3%; lateral up, 55.7%) (Table 3, Fig. 11C), while only one specimen (from HF24) was found in a dorsal up position (data not included in analysis due to different time of observation).

PeerJ Preprints | https://doi.org/10.7287/peerj.preprints.2707v1 | CC BY 4.0 Open Access | rec: 6 Jan 2017, publ: 6 Jan 2017

With respect to the classification of "time since death", 68.8% of the carcasses were classified in class 1 (less than 3 months), 24.9% in class 2 (less than 6 months) and 6.3% in class 3 (more than a year) (Fig. 11A-B, Table 4). With respect to "time at sea", 147 (87%) of the carcasses were classified in class A (short time/distance of drift), while only four (13%) were identified as class B (long time/distance of drift) (Fig. 11 C, Table 4). There was no pattern relating the geomorphological unit (sandy: 34%, pebble: 27%, rocky beach: 34%) to the taphonomic classes.

The carcasses found in April in Estero Slight were classified in stage 2 of Geraci and Lounsbury (2005) indicating a few days to weeks since death; this would be classified as class 1 in the taphonomic classes of the present study.

The density of whale carcasses was in average $1050/km^2$, considering all assemblages recognized (Table 5).

Carcass drift and potential source locations

PeerJ Preprints | https://doi.org/10.7287/peerj.preprints.2707v1 | CC BY 4.0 Open Access | rec: 6 Jan 2017, publ: 6 Jan 2017

The distribution of beached carcasses was simulated from four illustrative source locations (Fig. 12A-D). In each case, calculations tracked 13000 hypothetical carcasses, reflecting source times spanning a 2-month period from mid-February to mid-April 2015 and a range of drift model parameters. The spread of stranding locations therefore represents variability of the current, wind and wave environment during this period as well as the uncertainty in model parameters and a diffusive component to the drift tracks. While each of the illustrated source locations leads to strandings distributed over several hundred kilometres of coastline, there are important differences in these distributions. A simulated source in Golfo Tres Montes (northern Golfo de Penas) leads to strandings throughout the Golfo de Penas (Fig. 12A), including in the Golfo Tres Montes itself. No other source location (Fig. 12B-D) leads to strandings in Golfo Tres Montes due to the direction of prevailing currents and the sheltering effect of Peninsula Taitao. Similarly, only a source to the north of Peninsula Taitao leads to strandings in that region (Fig. 12B). Carcasses originating in the Golfo de Penas have a tendency to be transported to the south by prevailing currents (Fig. 12A, C, D).

Inter-annual variation in upwelling or downwelling

PeerJ Preprints | https://doi.org/10.7287/peerj.preprints.2707v1 | CC BY 4.0 Open Access | rec: 6 Jan 2017, publ: 6 Jan 2017

Comparison between the cumulative alongshore wind stress for the year in question and the previous 20 years (Fig. 13) reveals that the months immediately prior to the mortality event were anomalous. North of the study area, at 45°S, there was an anomalously strong tendency toward upwelling (an upward trend in Fig. 13), making this one of the most upwelled years of the period. At the latitude of Golfo de Penas and further south there was a net tendency to downwelling (a downward trend in Fig. 13), but punctuated by upwelling events, making this one of the least downwelled years of the period.

DISCUSSION

Possible causes of death (Table 6) need to be analysed for a mechanism that is capable of synchronous killing of hundreds of whales, apparently all or most of the same species (with few exceptions, i.e. one confirmed pinniped). Baleen whales, in contrast to odontocetes, are less social and do not use echolocation to navigate (Perrin et al., 2009b). The latter characteristics are key aspects used to explain mass mortalities in odontocetes.

Possible causes for the death of hundreds of baleen whales include a lethal and highly contagious unknown virus or infection, noise-related mechanisms at sea, and intoxication by biotoxins (domic acid, saxitocin, etc; Geraci et al., 1989; Fire et al., 2010; Lefebvre et al., 2016; Pyenson et al. 2014, Table 6). In this assemblage the individuals could not be tested for viruses or bacteria, due to their advanced state of decomposition. There was no evidence of pathological modifications that could be attributed to such a cause, however, it is not possible to completely discard this hypothesis.

PeerJ Preprints | https://doi.org/10.7287/peerj.preprints.2707v1 | CC BY 4.0 Open Access | rec: 6 Jan 2017, publ: 6 Jan 2017

The only potentially lethal noise-related mechanism for a baleen whale are very intense noises associated with blasting in close proximity (Ketten 1992). This could injure the animal and cause haemorrhage or provoke panic, disorientation and favour entrapment (not yet described for baleen whales, Goldbogen et al. 2013). Although there was no evidence of bony damage or micro-fracture of the one examined periotic, this cannot be excluded for the other individuals. Any other noise-related damage could neither be ruled out due to the decomposition of the soft tissue structures, nevertheless there is no evidence that for baleen sonar and ground noise could trigger more than non-lethal behavioural and temporary effects (Goldbogen et al. 2013). The strongest argument against this hypothesis is that whales died synchronously along hundreds of kilometres of shore line and at least five different sources of carcasses were identified (see discussion on drift models), which could only be explained by a large number of blastings along the coast during a very restricted time period. The study carried out by SERNAPESCA (Fiscalía de Aysén, 2015; Ulloa et al., 2016, available upon request from SERNAPESCA authorities) based on partial necropsies of two whales in late May 2015, found no evidence of any trauma or human interaction. The whales were already in decomposition stage 3 to 4 and class 1 of taphonomic classes used here.

PeerJ Preprints | https://doi.org/10.7287/peerj.preprints.2707v1 | CC BY 4.0 Open Access | rec: 6 Jan 2017, publ: 6 Jan 2017

Paralytic shellfish toxin (PST) is known to accumulate in the pelagic stage of the squat lobster *Munida gregaria* (MacKenzie & Harwood, 2014), an important prey of sei whales (Matthews, 1932). Older reports (Tabeta & Kanamura, 1970) and recent observations by boat crews (pers. comm. Keri-Lee Pashuk, 2015) indicate that squat lobster abundance fluctuates strongly and can reach extremely high concentrations, especially in Golfo Tres Montes (Tabeta & Kanamura, 1970). The presence of PST in mytilids from the area and in the whale carcasses and the absence of evidence for other causes of death leaves paralytic shellfish poisoning (PSP) as the most probable cause of death (Table 6). Although AST was also detected in one of the stomach content samples, it is not believed to be the cause of the MME as it was not detected by the toxin monitoring stations. A mixed assemblage of 40 skeletons from the Miocene in the north of Chile, dominated by rorqual whales and attributed to four recurrent HAB events, shows many similarities to the assemblages described here (Pyenson et al., 2014). The characteristics of the MME and the repetition in the same locality are common features for HAB-mediated mortalities (Brongersma-Sanders, 1957) (see Table 6, 7). MMEs through PSP in rorquals are thus not a recent phenomenon in the South East Pacific. Nevertheless, whale bone accumulations and reports of mortalities in Chilean Patagonia of up to 15 rorquals going back to at least 1977 suggest an increase in the frequency of mortalities (Table 8). Since the early 1990s HABs have been recorded every year in spring and autumn along the entire Patagonian coast but patterns are patchy and generally restricted to bays and fjords. The same is true the coast of the Northeast Pacific where HAB events have been increasing in strength and extension (Cook et al., 2015). This MME coincided with increased mortality of baleen whales along the west coast of North America in 2015 (NOAA, 2015b), and with the most extended and longest lasting HAB event registered there (NOAA, 2015c). A positive correlation between the occurrence of PST

PeerJ Preprints | https://doi.org/10.7287/peerj.preprints.2707v1 | CC BY 4.0 Open Access | rec: 6 Jan 2017, publ: 6 Jan 2017

51

blooms and the ENSO indices in northern and central Patagonia has been shown (Cassis et al., 2002; Guzmán & Pizarro, 2014). A similar correlation between the abundance of toxic harmful algae and surface temperatures, which in turn are affected by ENSO, was observed in Aysén by Cassis et al., (2002). El Niño events have increased in frequency and strength due to global warming (Cai et al., 2014). A strong El Niño event began to build in September 2014, which became the strongest El Niño of all time (NOAA, 2015a). The calculated cumulative windstress (Fig. 13) suggests that during this period there was an anomalous tendency towards coastal upwelling and associated nutrient delivery. Exceptionally high levels of PST, ten times higher than usual peaks, were reported in March 2015 from the closest monitoring site 120km north of the mortality area (Isla Canquenes, Fig. 14).

The presence of PST during February 2016 was accompanied by deep red/brown surface water discoloration due to the high abundance of *Alexandrium catenella*. This harmful algal bloom was coincidental with an unusually large bloom of the same toxic species in the waters around Chiloé island (42°S) (Hernández et al, 2016). The May 2016 expedition did not observe water discolouration at this location, nevertheless the phytoplankton samples obtained at the mouth of Seno Newman were also positive for PST, indicating that this toxic species can be present in the area for long periods of time during the summer. The PST levels at Isla Canquenes were not elevated in 2016; however, at two sites in the Messier Channel levels four and seven times higher than usual peaks, were measured (Fig. 15)

52

Rorqual whales sink shortly after death (Smith et al., 2015). Once carcasses have sunk below a depth of 50 m to 100 m, they tend not to re-float since hydrostatic pressure compresses decomposition gases (Smith et al., 2015). The bathymetry in the Golfo de Penas area and off the steeply sloping Taitao Peninsula (Fig. 12) requires that the whales that washed ashore all died near the shore. Thus, we conclude that despite common belief (Perrin et al., 2009a) sei whales opportunistically feed close to shore and may even follow their prey into narrow and shallow inlets and channels. This hypothesis is supported by the fact that live Sei whales were observed nearshore in Golfo de Penas and Estero Slight on several occasions (Table 8).

PeerJ Preprints | https://doi.org/10.7287/peerj.preprints.2707v1 | CC BY 4.0 Open Access | rec: 6 Jan 2017, publ: 6 Jan 2017

The drift model suggests that the observed carcasses originated from multiple sites. The carcasses found in the two fjordic inlets of Seno Newman and Estero Slight (62% of the total) probably died not far from where they stranded, either in the Golfo Tres Montes or within the inlets themselves (Figs. 1, 9), since source locations elsewhere in Golfo de Penas or north of Taitao Peninsula do not lead to carcasses in this region (Fig. 12B-D). Although the inlets themselves are not resolved in the drift model, the net seaward surface outflow of a fjord would only allow carcasses to collect toward its head (as observed) if wind and waves in that direction dominated their drift, or if they died close to the site where they were found. Modeled winds were occasionally toward the head of Seno Newman, on March 20 and during April 14 -18, but almost never in the case of Estero Slight (Fig. 16), so it is highly likely that the carcasses found within these inlets were the result of mortality within the inlets themselves. Carcasses from within these inlets could, however, be exported to nearby coastal waters and then distributed around Golfo de Penas as seen in the drift simulations for a source in Golfo Tres Montes (Fig. 12A), so mortality within the inlets of Seno Newman and Estero Slight could have been the source for carcasses found elsewhere in Golfo Tres Montes or Golfo de Penas.

The accumulation of carcasses in the convoluted and extremely shallow Estero Escondido is similarly unresolvable by the drift model, but it also appears highly likely that these carcasses resulted from mortality within the inlet itself. It is however unclear why dozens of large whales would swim into a narrow inlet which in most parts is only between 2 and 7 m deep (maximum depth 15 m just inside extremely shallow entrance) (Fig. 17).

PeerJ Preprints | https://doi.org/10.7287/peerj.preprints.2707v1 | CC BY 4.0 Open Access | rec: 6 Jan 2017, publ: 6 Jan 2017

Drift predictions from sources within Golfo de Penas, or to the south (Fig. 12A, C-D), never led to carcasses on or to the north of Taitao Peninsula, therefore the observed carcasses on the exposed shoreline in that region (Estero Cono) likely originated close to shore, either locally or to the north. The carcasses found between the southern end of Golfo de Penas and 49°S either died very close to where they washed ashore or were transported from the large concentrations in Golfo de Penas by clockwise flow within the gulf. The five whales between 49°S and 51°S probably died locally.

Surveys in the Golfo de Penas area have sighted sei whales in all seasons, with up to 600 individuals, some even near to the shore of Golfo de Penas and Estero Slight (Table 8). Therefore, the number of whales that have been exposed to toxins could be considerable. It has been calculated that less than 10% of the gray whales that are estimated to die each year in the eastern North Pacific are washed ashore, while most sink and do not resurface (Rugh et al., 1999). Assuming a similar ratio, our observations may greatly underestimate the actual magnitude of this mortality event. Many whales may have sunk and never re-surfaced, and a significant number of carcasses may have been washed ashore on the many remote beaches that could not be surveyed due to adverse weather conditions. Others may have been destroyed by wave action from winter storms on the high-energy rocky shores that dominate the area.

In other reported MMEs, the period of the time of a massive mortality was determined by considering the number of carcasses, and their temporal and spatial extent. This ranged from two years (gray whales; Gulland et al., 2005) to a few weeks (Humpback whales of cape Code; Geraci, 1989). To determine the time span of this MME, the classification of carcasses was carried out following the disarticulation sequence proposed by Schäfer (1972).

PeerJ Preprints | https://doi.org/10.7287/peerj.preprints.2707v1 | CC BY 4.0 Open Access | rec: 6 Jan 2017, publ: 6 Jan 2017

Time since death and time of transportation at sea of the carcass are slightly different in terms of articulation and state of decomposition. Following Schäfer (1972), the first breakage of the outer tissue of a carcass at sea should occur within a week to a month, although in Chilean Patagonia the time span could be a little greater due to the low temperature. In addition, some carcasses could have drifted for some weeks, arrived intact on shore, and then decayed more rapidly exposing the bones, while other carcasses could have floated longer until skull, tail and limbs were disarticulated, but decayed more slowly due to the colder water temperatures. This was in agreement with the comparisons of the disarticulation of carcasses in the field assessed through the photographs of the different expeditions to the same area (Estero Slight, in April and May 2015). Nevertheless, at the present assemblage, the time until the bones were exposed was extended from 1 to around 3 months (class 1) and time of disarticulation was shifted from 3 to 6 months (class 2), due to the low average temperature in the study area.

Considering available information on MMEs time scales, it is reasonable to suppose this event occurred over a time span of approximately three to maximum six months (November 2014 to April 2015). Nevertheless, the record of other crews (Table 2) and modeled oceanographic conditions (see "Carcass drift and potential source locations", above) point to the beginning of the die off around February at Golfo de Penas. Thus the class 2 carcasses would indicate another pulse of corpses arriving at the same area in a different taphonomic condition, which could suggest: a) longer drift time/distance transport; b) equal arrival but different time of death; or c) higher energy environment. The classification of "time at sea" analysis suggested that drift time was in its majority the same with a similar proportion of class a (short drift time/distance). The analysis of the anatomic positions suggests the allochthonous nature of the deposits in all assemblages (see Pyenson et al., 2014). Only two carcasses were found in a dorsal up position which suggests live stranding.

The average density of Golfo Tres Montes assemblages is equivalent to one third of the density calculated for Cerro Ballena, a Late Miocene (~9 m.y.a.) fossil red tide linked assemblage of northern Chile (3000/km^2, Pyenson et al., 2014) (Table 5). However, this difference is likely to have a sampling bias since in Golfo Tres Montes and Golfo de Penas we could only could the carcasses along the coastline, but not on the seafloor.

CONCLUSIONS

PeerJ Preprints | https://doi.org/10.7287/peerj.preprints.2707v1 | CC BY 4.0 Open Access | rec: 6 Jan 2017, publ: 6 Jan 2017

1. The whales died at sea, close to where they beached. About 90% of the whales died during one MME (94.7% for time since death and 87% for time at sea analysis), most probably between February and April 2015. No major mortality has occurred in the same area in 2016, but mortalities in other areas cannot be excluded (see Fig. 15 for 2016 toxin levels).
2. Since it is likely that all or most of the affected whales were sei whales, the documented mortality may represent a significant increase over the usual death rate of Southern Hemisphere sei whales (Reilly et al., 2008). If the frequency and magnitude of MMEs increase due to climate change this would have a significant impact on the local population and threaten the recovery of this endangered species, which in the Southern Hemisphere was reduced by whaling from about 100,000 to 24,000 individuals by 1980 (Perrin et al., 2009a).
3. This MME and historical data suggest that, at least during years with abundant squat lobsters, the Golfo de Penas is one of the most important feeding grounds for sei whales, hosting the largest and densest known sei whale aggregations outside the polar regions.
1. The MME reported herein and its probable connection to El Nino-caused red tide events throughout the eastern Pacific could indicate that marine mammals are among the first oceanic megafauna victims of global warming.

4. Discoveries of dead whales in this remote area are chance finds. To clarify the extent, frequency and magnitude of MMEs, an assessment and systematic monitoring of whale populations in Central Chilean Patagonia is necessary. We suggest to do this through regular satellite images.

PeerJ Preprints | https://doi.org/10.7287/peerj.preprints.2707v1 | CC BY 4.0 Open Access | rec: 6 Jan 2017, publ: 6 Jan 2017

Acknowledgements

We particularly thank the organizers and participants of the expedition organized by the Chilean Fisheries Service (SERNAPESCA), especially B. Caceres, G. Garrido, M. Ulloa, F. Viddi, J. Acevedo, T. García, C. Calderón and L. Bedriñana. Thanks also to R. Brownell, N. Pyenson, L. Pastene, E. Poulin, F. Beaujot, U. Pörschmann, P. Pascoe, S. Kraft, K.-L. Pashuk and V. Beasley. Thanks to Bidema PDI, Fiscalía de Aysén and Armada de Chile for field support. We are thankful to many more people for assisting with field-work, technical support and logistics, for sharing or facilitating data and information, and for discussions. This is publication number 134 of Huinay Scientific Field Station.

References

Aguayo-Lobo A. 1974. *The whale problem: a status report*. Cambridge, Massachusetts: Harvard University Press.

Anonymous. 2015. Report of the second workshop on mortality of Southern right whales (*Eubalaena australis*) at Península Valdés, Argentina. Report SC/66a/Rep/9 presented to the Scientific Committee meeting, San Diego, 20th May - 4th June.

Ardhuin F, Marié L, Rascle N, Forget P, and Roland A. 2009. Observation and estimation of Lagrangian, Stokes, and Eulerian currents induced by wind and waves at the sea surface. *Journal of physical oceanography* 39:2820–2838.

Baker CS, and Clapham PJ. 2004. Modelling the past and future of whales and whaling. *Trends in Ecology & Evolution* 19:365–371.

Breivik Ø, Allen A, Maisondieu C, Roth JC, and Forest B. 2012. The leeway of shipping containers at different immersion levels. *Ocean Dynamics* 62:741–752.

Behrensmeyer, AK. 1973. The taphonomy and paleoecology of Plio-Pleistocene vertebrate assemblages east of Lake Rudolf, Kenya. Harvard University.

Brongersma-Sanders M. 1957. Mass mortality in the sea. *Geological Society of America Memoirs* 167:941–1010.

Cai W, Borlace S, Lengaigne M, van Rensch P, Collins M, Vecchi G, Timmermann A, Santoso A, McPhaden MJ, Wu L, England MH, Wang G, Guilyardi E, and Jin F-F. 2014. Increasing frequency of extreme El Niño events due to greenhouse warming. *Nature Climate Change* 4:111–116. 10.1038/nclimate210

Cassis D, Muñoz P, and Avaria S. 2002. Variación temporal del fitoplancton entre 1993 y 1998 en una estación fija del seno Aysén, Chile (45º26′S 73º00′W). *Revista de Biología Marina y Oceanografía* 37:43–65.

Clapham PJ, Young SB, and Brownell RL. 1999. Baleen whales: conservation issues and the status of the most endangered populations. *Mammal review* 29:37–62.

Cook PF, Reichmuth C, Rouse AA, Libby LA, Dennison SE, Carmichael OT, Kruse-Elliott KT, Bloom J, Singh B, Fravel VA, Barbosa L, Stuppino JJ, Van Bonn WG, Gulland FMD, and Ranganath C. 2015. Algal toxin impairs sea lion memory and hippocampal connectivity, with implications for strandings. *Science* 350:1545–1547. 10.1126/science.aac5675

Coughran DK, Gales NJ, and Smith HC. 2013. A note on the spike in recorded mortality of humpback whales (*Megaptera novaeangliae*) in Western Australia. *Journal of Cetacean Research and Management* 13:105–108.

D'Agostino VC, Hoffmeyer MS, Almandoz GO, Sastre V, and Degrati M. 2015. Potentially toxic Pseudo-nitzschia species in plankton and fecal samples of *Eubalaena australis* from Península Valdés calving ground, Argentina. *Journal of Sea Research* 106:39–43. DOI: 10.1016/j.seares.2015.09.004

Dalebout M, Robertson K, Frantzis A, Engelhaupt D, Mignucci- Giannoni A, RosarioDelestre R, Baker CS. 2005. Worldwide structure of mtDNA diversity among Cuvier's beaked whales (*Ziphius cavirostris*): implications for threatened populations. *Molecular Ecology* 14:3353–3371.

Dee DP, Uppala SM, Simmons AJ, Berrisford P, Poli P, Kobayashi S, Andrae U, Balmaseda MA, Balsamo G, Bauer P, and Bechtold P. 2011. The ERA−Interim reanalysis: Configuration and performance of the data assimilation system. *Quarterly Journal of the Royal Meteorological Society* 137:553-597.

Doucette GJ, Cembella AD, Martin JL, Michaud J, Cole TVN, and Rolland RM. 2006. Paralytic shellfish poisoning (PSP) toxins in North Atlantic right whales *Eubalaena glacialis* and their zooplankton prey in the Bay of Fundy, Canada. *Marine Ecology Progress Series* 306:303-313.

Durbin E, Teegarden G, Campbell R, Cembella A, Baumgartner MF, and Mate BR. 2002. North Atlantic right whales, *Eubalaena glacialis*, exposed to paralytic shellfish poisoning (PSP) toxins via a zooplankton vector, *Calanus finmarchicus*. Harmful Algae 1:243–251.

Fire SE, Wang Z, Berman M, Langlois GW, Morton SL, Sekula-Wood E, and Benitez-Nelson, CR. 2010. Trophic transfer of the harmful algal toxin domoic acid as a cause of death in a minke whale (*Balaenoptera acutorostrata*) stranding in southern California. *Aquatic Mammals*, *36*(4):342-350.

Fiscalía de Aysen. 2015. Official request SIAC nr 460428815 for report, Hucke-Gaete R, Viddi F, Cassis D, Bedriñana L, Häussermann V, Pérez-Alvarez MJ, Horwitz FE, Gutstein CS, Garrido-Toro G, Cáceres B, Aguayo A, Ulloa M. Inédito. Informe técnico sobre la mortalidad masiva de ballenas en Puerto Slight y Caleta Buena, Golfo de Penas, Región de Aysén (expedición de mayo 2015).

Försterra G. 2009. Ecological and Biogeographical Aspects of the Chilean Fjord Region, p. 61–76. In: Häussermann, V. & Försterra, G. (eds): Marine Benthic Fauna of Chilean Patagonia, Nature in Focus, Puerto Montt, 1000 pp.

PeerJ Preprints | https://doi.org/10.7287/peerj.preprints.2707v1 | CC BY 4.0 Open Access | rec: 6 Jan 2017, publ: 6 Jan 2017

Försterra G, Häussermann V and Laudien J. In press. Animal forests in the Chilean fjords: discoveries, perspectives and threats in shallow and deep waters. In: Rossi S, Bramanti L, Gori A, Orejas Saco del Valle C (eds.): Marine animal forests - The Ecology of Benthic Biodiversity Hotspots. Springer International Publishing.Geraci JR, Anderson DM, Timperi RJ, Early GA, Prescott JH, and Mayo CA. 1989. Humpback whales (*Megaptera novaeangliae*) fatally poisoned by dinoflagellate toxin. *Journal of the Fisheries Research Board of Canada* 46:1895–1898.

Geraci JR, and Aubin DJ. 1977 Mass stranding of the long-finned pilot whale, *Globicephala melaena*, on Sable Island, Nova Scotia. *Journal of Fisheries Research Board of Canada* 34, 2193 – 2196. DOI 10.1139/f77-288.

Geraci JR, and Lounsbury VJ. 2005. Marine Mammals Ashore: A Field Guide for Strandings Second Edition. National Aquarium in Baltimore. Baltimore, MD.

Geraci JR, Anderson, DM, Timperi RJ, St. Aubin DJ, Early GA, Prescott JH, and Mayo CA. 1989. Humpback whales (*Megaptera novaeangliae*) fatally poisoned by dinoflagellate toxin. Canadian Journal of Fisheries and Aquatic Sciences, 46:1895-1898.

Gilmore RM. 1971. Observations on marine mammals and birds off the coast of southern and central Chile, early winter 1970. *Antarctic Journal of the United States* 6:10–11.

Goldbogen J.A, Southall B L, DeRuiter SL, Calabokidis J, Friedlaender AS, Hazen E L, Falcone EA, Schorr GS, DouglasA, Moretti D, Kyburg C, McKenna M F, Tyack PL. 2013. Blue whales respond to simulated mid-frequency military sonar. *Proceedings of the Royal Society – B Biological Sciences* 280: 20130657.

González H, Calderón M, Castro L, Clement A, Cuevas L, Daneri G, Iriarte J, Lizárraga L, Martínez R, and Menschel E. 2010. Primary production and plankton dynamics in the Reloncaví Fjord and the Interior Sea of Chiloé, Northern Patagonia, Chile. *Marine Ecology Progress Series* 402:13–30.

Gulland FMD, Pérez-Cortés H, Urban J, Rojas-Bracho L, Ylitalo G, Weir J, Norman SA, Muto MM, Rugh DJ, Kreuder C, and Rowles T. 2005. Eastern North Pacific gray whale (*Eschrichtius robustus*) unusual mortality event, 1999-2000. NOAA Technical Memorandum NMFS-AFSC-150. p 44.

Guzmán L, Pacheco H, Pizarro G , and Alarcón C. 2002. *Alexandrium catenella* y veneno paralizante de los mariscos en Chile. In: Sar E, Ferrario M and Reguera B. (eds). Floraciones Algales Nocivas en el Cono Sur Americano, 235–255.Guzman L & Pizarro G. 2014. Effects of the El Niño-Southern Oscillation (ENSO) teleconnections on the abundance of micro-phytoplankton and *Alexandrium catenella*, in Southern Chile. Presented at the ICHA 16 conference in Wellington, New Zealand.

PeerJ Preprints | https://doi.org/10.7287/peerj.preprints.2707v1 | CC BY 4.0 Open Access | rec: 6 Jan 2017, publ: 6 Jan 2017

Häussermann V, and Försterra G. 2005. Distribution patterns of Chilean shallow-water sea anemones (Cnidaria: Anthozoa: Actiniaria, Corallimorpharia); with a discussion of the taxonomic and zoogeographic relationships between the actinofauna of the South East Pacific, the South West Atlantic and Antarctica. P. 91–102. In Arntz WE, Lovrich GA, and Thatje S (eds.): The Magellan-Antarctic connection: links and frontiers at high southern latitudes. Scientia Marina 69 (Suppl 2).Hernández C, Díaz PA, Molinet C, and Seguel M. 2016. Exceptional climate anomalies and northwards expansion of Paralytic Shellfish Poisoning outbreaks in southern Chile. Harmful Algae News 54: 1–2.Holz M, and Simões MG. 2002. Elementos fundamentais de tafonomia, Ed. Universidade, Porto Alegre, p. 231.

Jauniaux T, Charlier G, Desmecht M, Haelters J, Jacques T, Losson B, Van Gompel J, Tavernier J, and Coignoul, F. (2000). Pathological findings in two fin whales (Balaenoptera physalus) with evidence of morbillivirus infection. *Journal of comparative pathology*, *123*(2), 198-201. DOI: 10.1053/jcpa.2000.0395

Ketten DR. 1992. Estimates of blast injury and acoustic trauma zones for marine mammals from underwater explosions In: Kastelein RA, Thomas JA, and Nachtigall PE (eds.): Sensory Systems of Aquatic Mammals (1995) De Spil Publishers, Woerden, The Netherlands, ISBN 90-72743-05-9.

Kraus SD. 1990. Rates and potential causes of mortality in North Atlantic right whales (*Eubalaena glacialis*). *Marine Mammal Science* 6(4):278-91.

Large W G, and Pond S. 1981. Open ocean momentum flux measurements in moderate to strong winds. Journal of Physical Oceanography 11: 324–481.

PeerJ Preprints | https://doi.org/10.7287/peerj.preprints.2707v1 | CC BY 4.0 Open Access | rec: 6 Jan 2017, publ: 6 Jan 2017

Lefebvre KA, Quakenbush L, Frame E, Huntington KB, Sheffield G, Stimmelmayr G, Bryan A, Kendrick P, Ziel H, Goldstein T, Snyder JA, Gelatt T, Gulland F, Dickerson B, and Verena G. 2016. Prevalence of algal toxins in Alaskan marine mammals foraging in a changing arctic and subarctic environment. *Harmful Algae* 55: 13–24. DOI: 10.1016/j.hal.2016.01.007

Liebig PM, Taylor T-SA, and Flessa KW. 2003. Bones on the beach: marine mammal taphonomy of the Colorado Delta, Mexico. *Palaios* 18:168–175.

Liebig PM, Flessa KW, and Taylor SA. 2007 Taphonomic variation despite catastrophic mortality: analysis of a mass stranding of false killer whales (*Pseudorca crassidens*), Gulf of California, Mexico. *Palaios* 22, 384 – 391. DOI:10.2110/palo.2005.p05-052r)

MacKenzie AL, and Harwood T. 2014. Grazing on a toxic *Alexandrium catenella* bloom by the lobster krill *Munida gregaria* (Decapoda: Galatheoidea: Munididae). *Harmful Algae* 39:161–164.

Matthews LH. 1932. Lobster-krill. Anomuran crustacean that are the food of whales. *Discovery Reports* 5:467–484.

Mazzariol S, Centelleghe C, Beffagna G, Povinelli M, Terracciano G, Cocumelli C, Pintore A, Denurra D, Casalone C, Pautasso A, Di Francesco CE, and Di Guardo G. 2016. Mediterranean Fin Whales (*Balaenoptera physalus*) Threatened by Dolphin MorbilliVirus. *Emerging Infectious Diseases*, *22*(2), 302–305. DOI: 10.3201/eid2202.150882

Molinet C, Lafon A, Lembeye G, Moreno CA. (2003). Patrones de distribución espacial y temporal de floraciones de Alexandrium catenella (Whedon & Kofoid) Balech 1985, en aguas interiores de la Patagonia noroccidental de Chile. *Revista chilena de historia natural*, 76(4), 681-698. DOI: 10.4067/S0716-078X2003000400011.

Moore, MJ, Knowlton AR, Kraus SD, Mclellan WA, Bonde RK. 2004. Morphometry, gross morphology and available histopathology in North Atlantic right whale (*Eubalaena glacialis*) mortalities (1970-2002). *Journal of Cetacean Research and Management* 6:199-214.

NOAA. 2015a. Climate Dignostics Bulletin. *Available at http://www.cpc.noaa.gov/products/analysis_monitoring/enso_advisory/ensodisc.pdf* (accessed August, 2015).

NOAA. 2015b. NOAA declares deaths of large whales in Gulf of Alaska an unusual mortality event. *Available at http://alaskafisheries.noaa.gov/newsreleases/2015/whales-ume082015.htm* (accessed August, 2015).

NOAA. 2015c. NOAA fisheries mobilizes to gauge unprecedented West Coast toxic algal bloom. *Available at http://www.nwfsc.noaa.gov/news/features/west_coast_algal_bloom/index.cfm* (accessed June 2015).

Nowacek DP, Thorne LH, Johnston DW, Tyack PL. 2007 Response of cetaceans to anthropogenic noise. Mammal Review 37:81-115. DOI: 10.1111/j.1365-2907.2007.00104.x.

Pastene LA, and Shimada H. 1999. Report of a sighting survey in Chile's exclusive economic zone with comments on sei whale distribution. *Anales del Instituto de la Patagonia, Serie Ciencias Naturales* 27:51–62.

PeerJ Preprints | https://doi.org/10.7287/peerj.preprints.2707v1 | CC BY 4.0 Open Access | rec: 6 Jan 2017, publ: 6 Jan 2017

Peltier H, Dabin W, Daniel P, van Canneyt O, Dorémus G, Huon M, and Ridoux V. 2012. The significance of stranding data as indicators of cetacean populations at sea: Modelling the drift of cetacean carcasses. *Ecological Indicators* 18:278–290.

Perrin WF, Würsig B, and Thewissen JGM. 2009a. *Encyclopedia of marine mammals*. London: Academic Press.

Perrin WF, Mead JG, and Brownell JRL. 2009b. Review of the evidence used in the description of currently recognized cetacean subspecies. U.S. Department of Commerce, National Oceanic and Atmospheric Administration, National Marine Fisheries Service, Southwest Fisheries Science Center.

Pierce SD, Barth JA, Thomas RE, and Fleischer GW. 2006. Anomalously warm July 2005 in the northern California Current: Historical context and the significance of cumulative wind stress. *Geophysical Research Letters* 33 DOI: 10.1029/2006GL027149.

Pizarro G, Garrido C, Cárdenas C, Frangópulos M, Alarcón C, Guzmán L, Zamora C, and Pacheco H. 2011. Spatial distribution of *Alexandrium catenella* and paralytic toxins in the plankton and shellfishs between Penas Gulf and Trinidad Channel (Spring 2008). *Ciencia y Tecnologia del Mar* 34:5–24.

Pyenson ND, Gutstein CS, Parham JF, Le Roux JP, Chavarría CC, Little H, Metallo A, Rossi V, Valenzuela-Toro AM, Velez-Juarbe J, Santelli CM, Rogers DR, Cozzuol MA, and Suárez ME. 2014. Repeated mass strandings of Miocene marine mammals from Atacama Region of Chile point to sudden death at sea. *Proceedings of the Royal Society B-Biological Sciences* 281:20133316. DOI: 10.1098/rspb.2013.3316

Reilly SB, Bannister JL, Best PB, Brown M, Brownell Jr. RL, Butterworth DS, Clapham PJ, Cooke J, Donovan GP, Urbán J, and Zerbini AN. 2008. The IUCN Red List of Threatened Species. Version 2015.2. *Available at www.iucnredlist.org* (accessed 05 September 2015).

Rowntree VJ, Uhart MM, Sironi M, Chirife A, Di Martino M, La Sala L, Musmeci L, Mohamed N, Andrejuk J, McAloose D, Sala JE, Carribero A, Rally H, Franco M, Adler FR, Brownell Jr. RL, Seger J, Rowles T. 2013. Unexplained recurring high mortality of southern right whale *Eubalaena australis* calves at Península Valdés, Argentina. *Marine Ecology Progress Series* 493:275–289. DOI: 10.3354/meps10506

Rugh DJ, Muto M, Moore S, and DeMaster D. 1999. *Status review of the eastern north Pacific stock of gray whales*: US Department of Commerce, National Oceanic and Atmospheric Administration, National Marine Fisheries Service, Alaska Fisheries Science Center.

Schäfer, W. 1972. Ecology and Palaeoecology of Marine Environments. The University of Chicago Press, Chicago, 568 pp.

Shimizu Y, Ohishi K, Suzuki R, Tajima Y, Yamada T, Kakizoe Y, Bando T, Fujise Y, Taru H, Murayama T, and Maruyama T. Amino acid sequence variations of signaling lymphocyte activation molecule and mortality caused by morbillivirus infection in cetaceans. *Microbiology and immunology*, *57*(9), 624-632.

Simões MG, & Holz M. (2004). Tafonomia: processos e ambientes de fossilização.In: Carvalho, I. S. de (ed) Paleontologia, Rio de janeiro:Interciência 19-45.

Simmonds MP, and Isaac SJ. 2007. The impacts of climate change on marine mammals: early signs of significant problems. *Oryx* 41:19–26.

Skamarock, WC, Klemp JB. 2008. A time-split nonhydrostatic atmospheric model for weather research and forecasting applications. *Journal of Computational Physics* 227: 3465-3485.

Smith CR, Glover AG, Treude T, Higgs ND, and Amon DJ. 2015. Whale-fall ecosystems: recent insights into ecology, paleoecology, and evolution. *Marine Science* 7:571–596. Suárez B, and Guzmán L. 2005. Floraciones de algas nocivas: mareas rojas y toxinas marinas. Editorial universitaria: 80pp.

Southall BL, Bowles AE, Ellison WT, Finneran JJ, Gentry RL, Greene CR, Charles R, Kastak, D, Ketten DR, Miller JH, Nachtigall PE, Richardson WJ, Thomas JA, and Tyack, PL. 2009. Marine mammal noise exposure criteria: Initial scientific recommendations. *The Journal of the Acoustical Society of America*, *125*(4): 2517-2517. DOI: 10.1121/1.4783461

Tabeta O, and Kanamura S. 1970. On the post larva of *Munida gregaria* (Crustacea, Galatheida) in Penas Bay, Chile, with reference to mass occurrence in 1969. *Science Bulletin of the Faculty of Agriculture* 24:227–230.

Terrametrics. 2015. Google earth 7.1.5.1557. *Available at http://www.earth.google.com* (accessed October 2015).

Thiel M, Macaya EC, Acuña E, Arntz WE, Bastias H, Brokordt K, Camus PA, Castilla JC, Castro LR, Cortés M, Dumont CP, Escribano R, Fernandez M, Gajardo JA, Gaymer CF, Gomez I, González AE, González HE, Haye PA, Illanes JE, Iriarte JL, Lancellotti DA, Luna-Jorquera G, Luxoro C, Manriquez PH, Marín V, Muñoz P, Navarrete SA, Perez E, Poulin E, Sellanes J, Sepúlveda HH, Stotz W, Tala F, Thomas A, Vargas CA, Vasquez J, and Vega JMA. 2007. The Humboldt Current System of northern and central Chile. *Oceanography and Marine Biology: An Annual Review* 45:195–344.

Toots H, 1965. Sequence of disarticulation in mammalian skeletons. *Contributions to Geology University of Wyoming*, 4(1):37-39.

Torres R, Silva N, Reid B, and Frangopulos M. 2014. Silicic acid enrichment of subantarctic surface water from continental inputs along the Patagonian archipelago interior sea (41–56° S). *Progress in Oceanography* 129:50–61.

Van Bressem MF, Duignan PJ, Banyard A, Barbieri M, Colegrove KM, de Guise S, di Guardo G, Dobson A, Domingo M, Fauquier D. 2014. Cetacean Morbillivirus: Current Knowledge and Future Directions. *Viruses*. 6(12):5145-5181. DOI:10.3390/v6125145.

Vanderlann ASM and Taggart CT. 2007. Vessel collisions with whales: the probability of lethal injury based on vessel speed. *Marine Mammal Science* 23(1): 144–156.

Vidal O, Gallo Reynoso JP. 1996. Die offs of marine mammals and sea birds in the gulf of California, México. *Marine Mammal Science* 12:627–635.

Voorhies MR. 1969. Taphonomy and population dynamics of an early Pliocene vertebrate fauna, Knox County, Nebraska. *Contributions to Geology, University of Wyoming* Special Paper Nr 1:1–69.

PeerJ Preprints | https://doi.org/10.7287/peerj.preprints.2707v1 | CC BY 4.0 Open Access | rec: 6 Jan 2017, publ: 6 Jan 2017

Wallcraft AJ, Metzger EJ, and Carroll SN. 2009. Software Design Description for the HYbrid Coordinate Ocean Model (HYCOM), Version 2.2. Report no. NRL/MR/7320--09-9166, Naval Research Laboratory, Stennis Space Center, Mississippi, USA.

Wilson C, Sastre AV, Hoffmeyer M, Rowntree VJ, Fire SE, Santinelli NH, Díaz Ovejero S, D'Agostino V, Marón CF, Doucette GJ, Broadwater MH, Wang Z, Montoya N, Seger J, Adler FR, Sironi M, and Uhart MM. 2015. Southern right whale (*Eubalaena australis*) calf mortality at Península Valdés, Argentina: Are harmful algal blooms to blame? *Marine Mammal Science* DOI:12263. 10.1111/mms.12263

Figure and table captions

Fig. 1: Location of dead whales and skulls found in Chilean Patagonian. Boat track: green (HF24), flight track: blue (HF25) A) Golfo de Penas, B) Golfo Tres Montes, C) Seno Escondido.

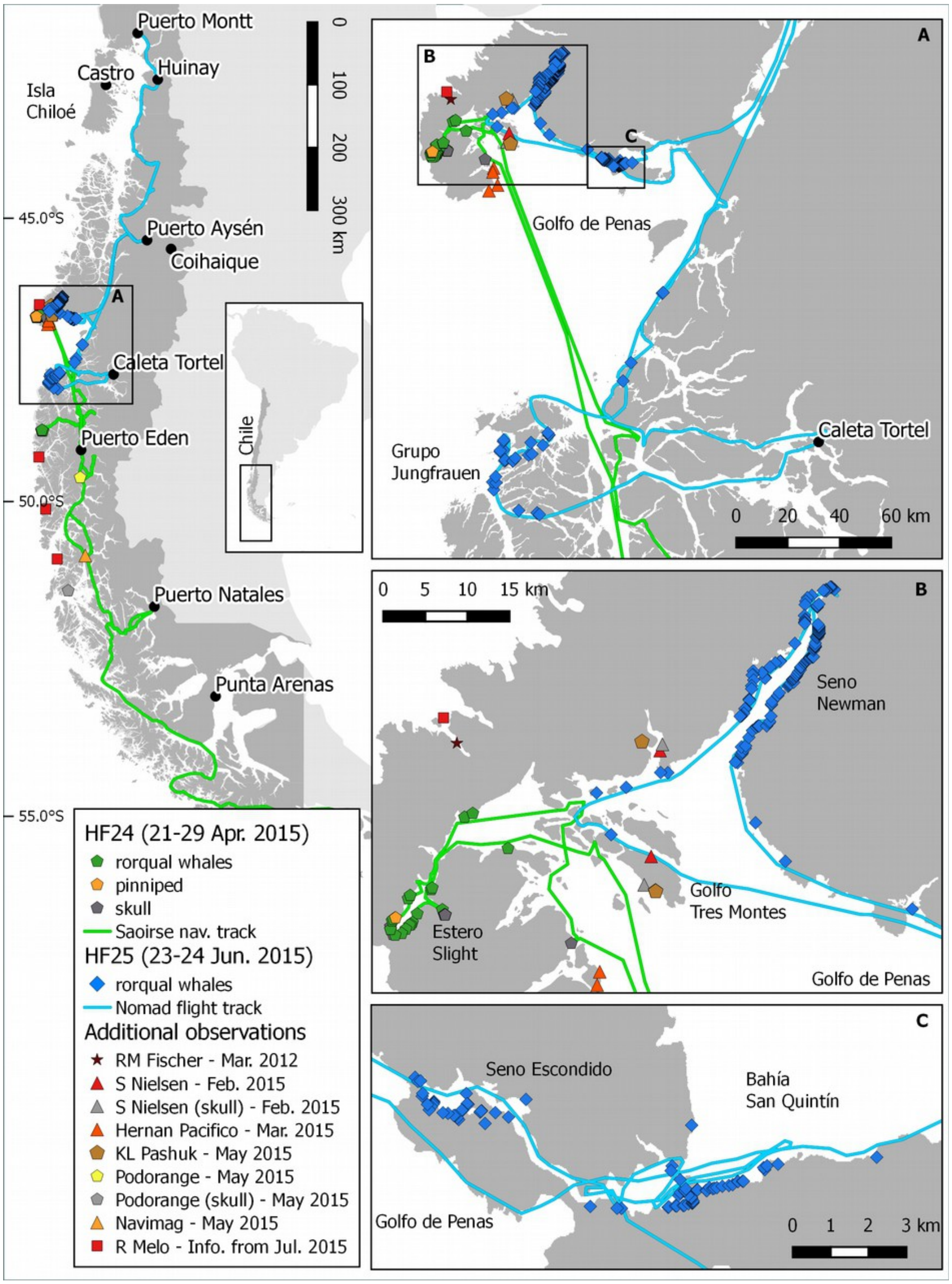

Fig. 2: Satellite image (MODIS Aqua) showing the concentration of chlorophyll a on March 23rd, 2015. Areas where most whales were found are circled.

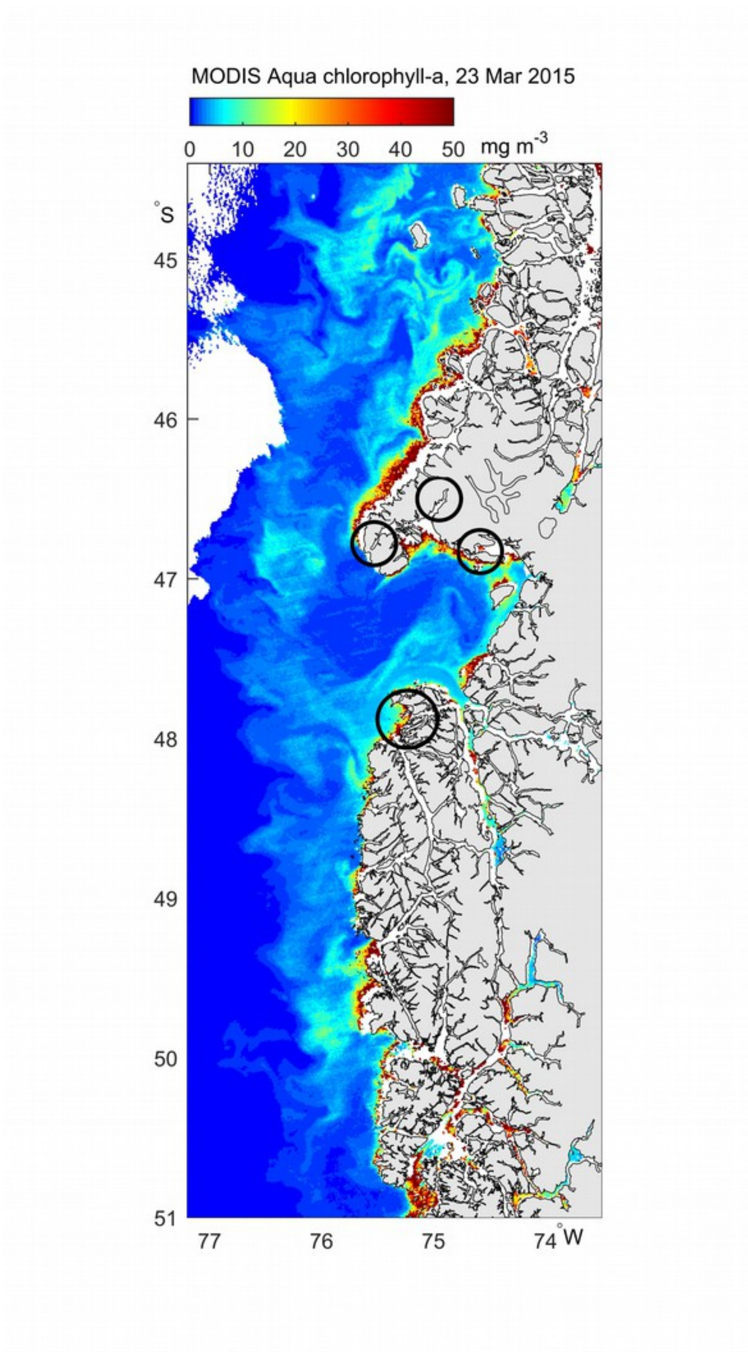

PeerJ Preprints | https://doi.org/10.7287/peerj.preprints.2707v1 | CC BY 4.0 Open Access | rec: 6 Jan 2017, publ: 6 Jan 2017

Fig. 3: Documented whale carcasses and skeletal remains during a vessel survey in April 21st 2015 in Caleta Buena, Estero Slight. A) and B) skeletal remains C) Recently dead sei whale. Photos: Keri-Lee Pashuk, all rights reserved.

PeerJ Preprints | https://doi.org/10.7287/peerj.preprints.2707v1 | CC BY 4.0 Open Access | rec: 6 Jan 2017, publ: 6 Jan 2017

Fig. 4: Documented whale carcasses and skeletal remains during an overflight on June 25st 2015, Seno Escondido. The numbers correspond to the whale identification numbers in Table 1. Photos: Vreni Häussermann, all rights reserved.

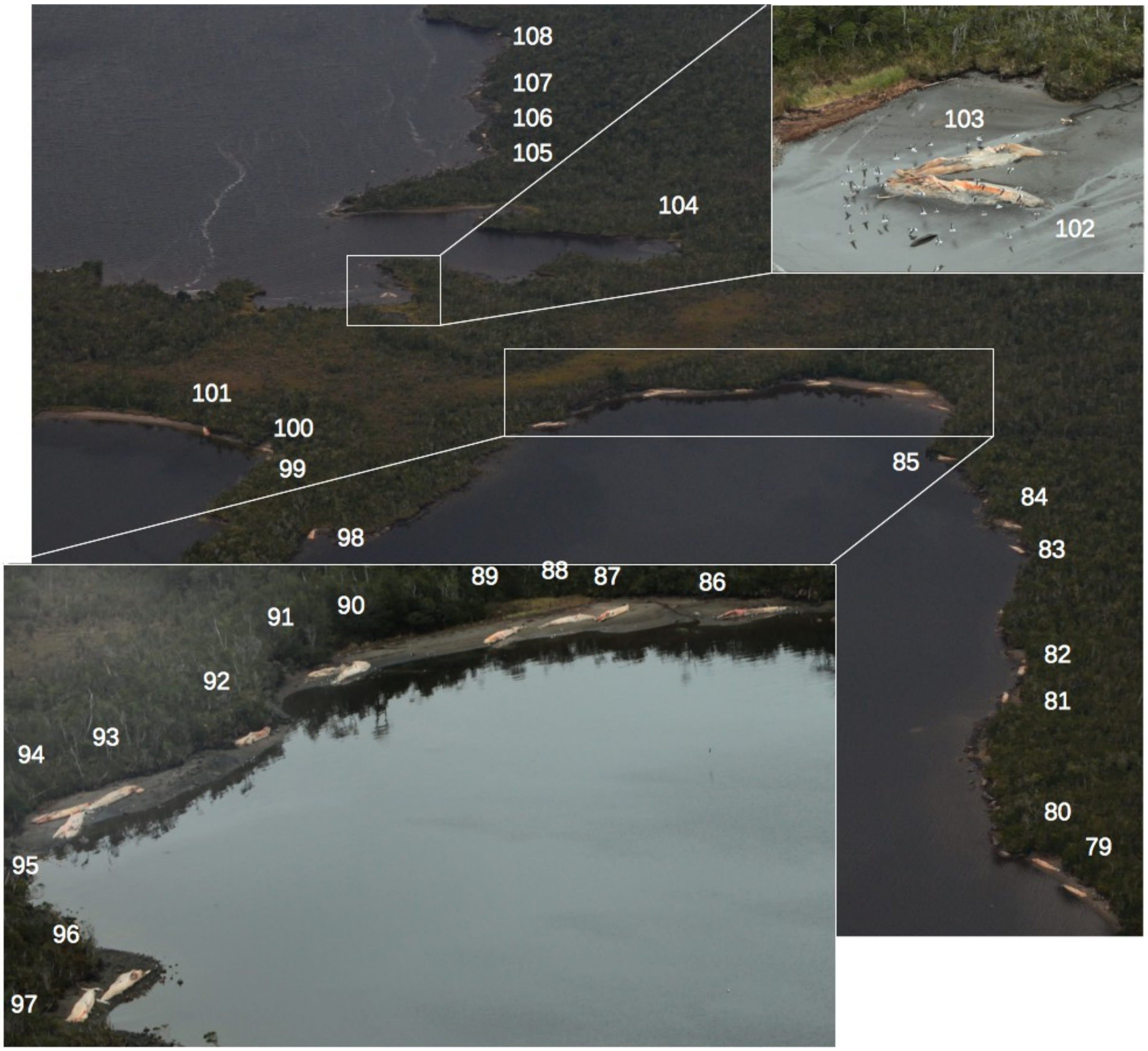

PeerJ Preprints | https://doi.org/10.7287/peerj.preprints.2707v1 | CC BY 4.0 Open Access | rec: 6 Jan 2017, publ: 6 Jan 2017

Fig. 5: A. A. Satellite image on August 13th 2015, used to count the carcasses along Seno Newman. B-C-D. Detail of the carcasses highlighted in A.

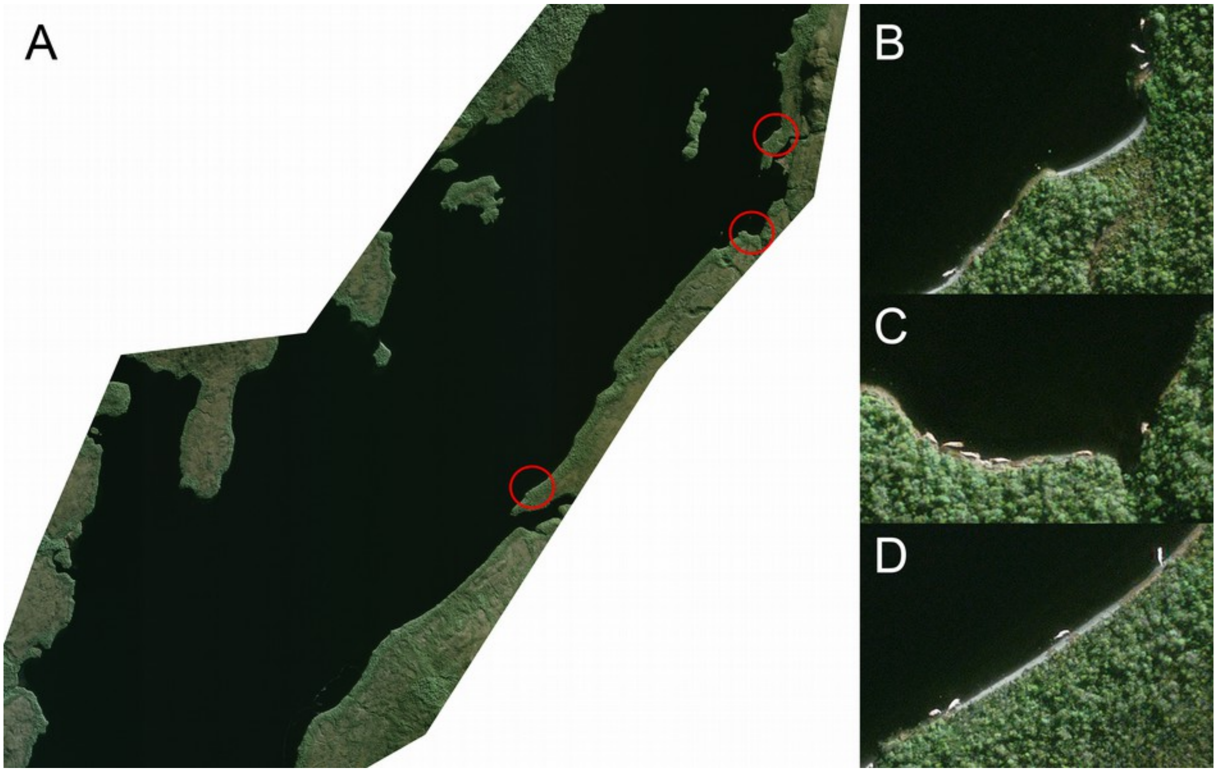

PeerJ Preprints | https://doi.org/10.7287/peerj.preprints.2707v1 | CC BY 4.0 Open Access | rec: 6 Jan 2017, publ: 6 Jan 2017

Fig. 6: Biostratinomic classification addressing the decomposition/desarticulation of carcasses/skeletal remains assessing to the time since death. A-B) Class 1, carcasses in the lowest to relatively medium state of decomposition, C-D) Class 2, carcasses in a relatively greater state of decomposition, but still maintaining their longitudinal axis, although some bones may be scattered, E-F) Class 3, isolated skeletal remains with no soft tissue.

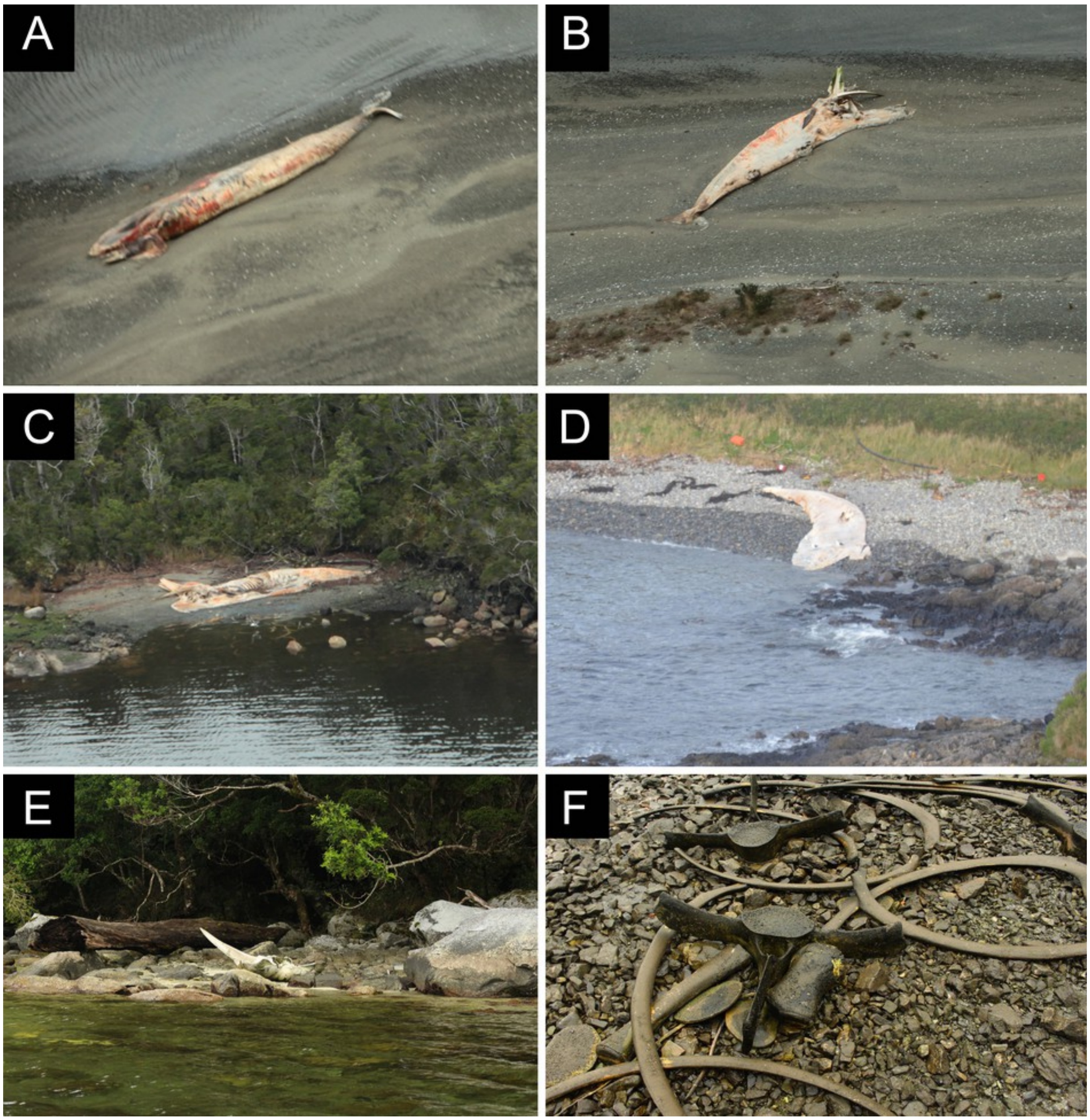

PeerJ Preprints | https://doi.org/10.7287/peerj.preprints.2707v1 | CC BY 4.0 Open Access | rec: 6 Jan 2017, publ: 6 Jan 2017

Fig 7: Biostratonomic classification of the location of death of carcasses/skeletal remains A) Carcasses preserving the skull, B) Carcasses lacking the skull.

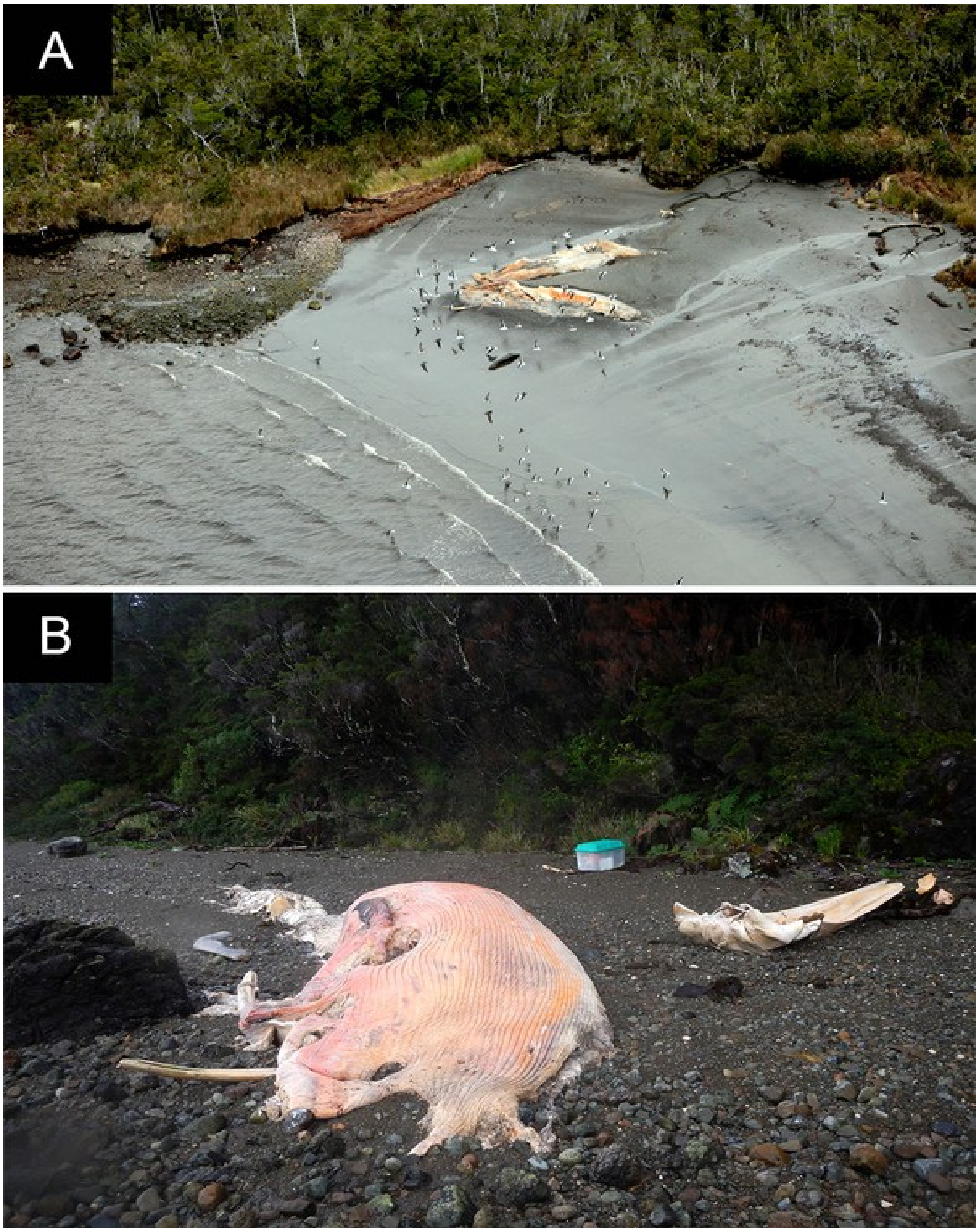

Fig. 8: Digital images obtained through computed volumetric tomography (CVT) scanned at Morita Tomography (box of 60 mm, 500 slices). All acoustic anatomical structures of the middle ear (ossicles: stapes), internal ear (cochlea: spiral lamina) and the semicircular canals are seen in perfect condition.

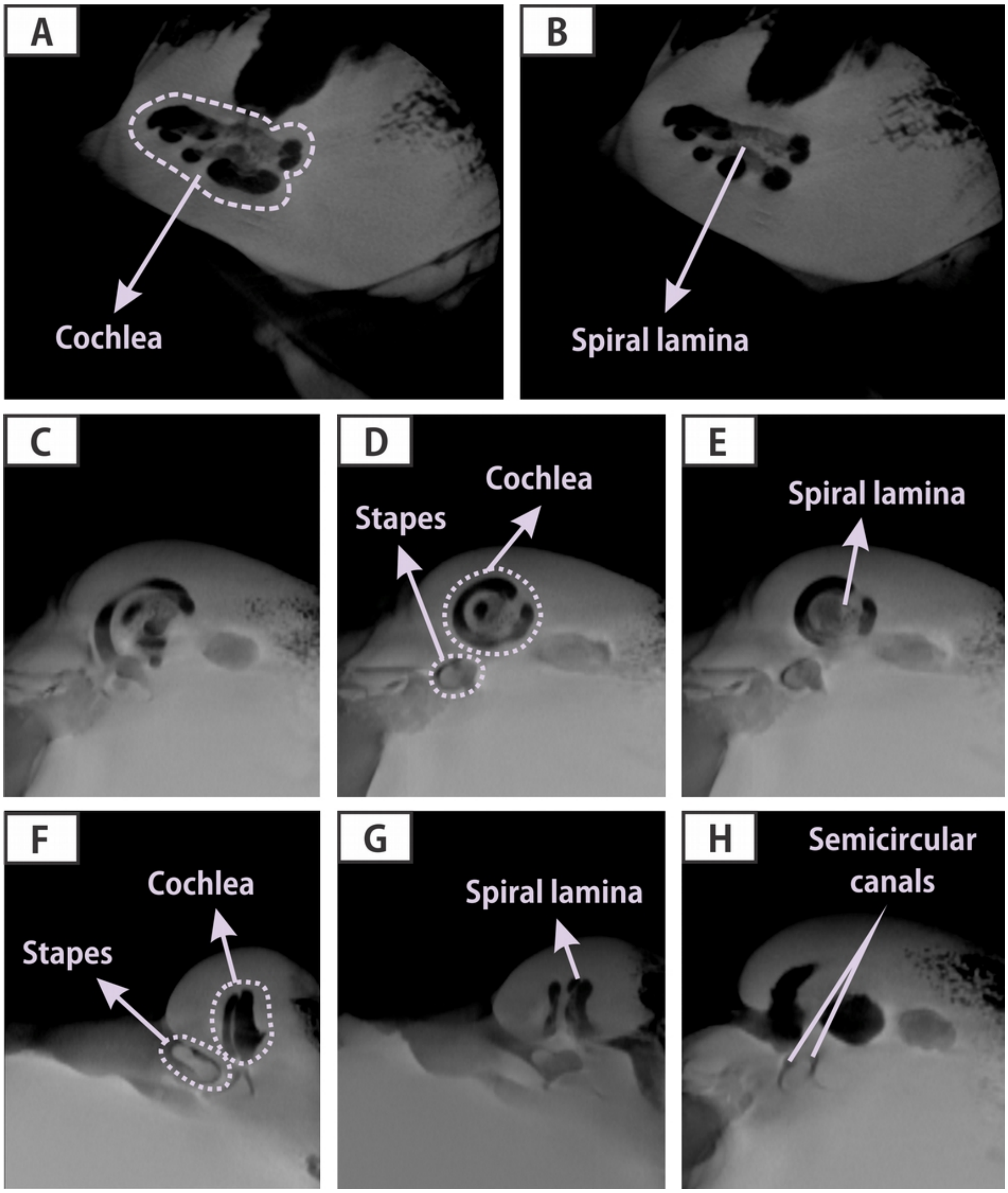

PeerJ Preprints | https://doi.org/10.7287/peerj.preprints.2707v1 | CC BY 4.0 Open Access | rec: 6 Jan 2017, publ: 6 Jan 2017

Fig. 9: Maps showing the five assemblages of whale carcasses. (A) Golfo de Penas, (B) Seno Escondido, (C) Seno Newman, (D) Estero Slight, (E) Jungfrauen Islands. State of decomposition color-coded: Yellow (state 1; least decomposed, all articulated), orange (state 2, intermediate decomposed), red (state 3; isolated remains).

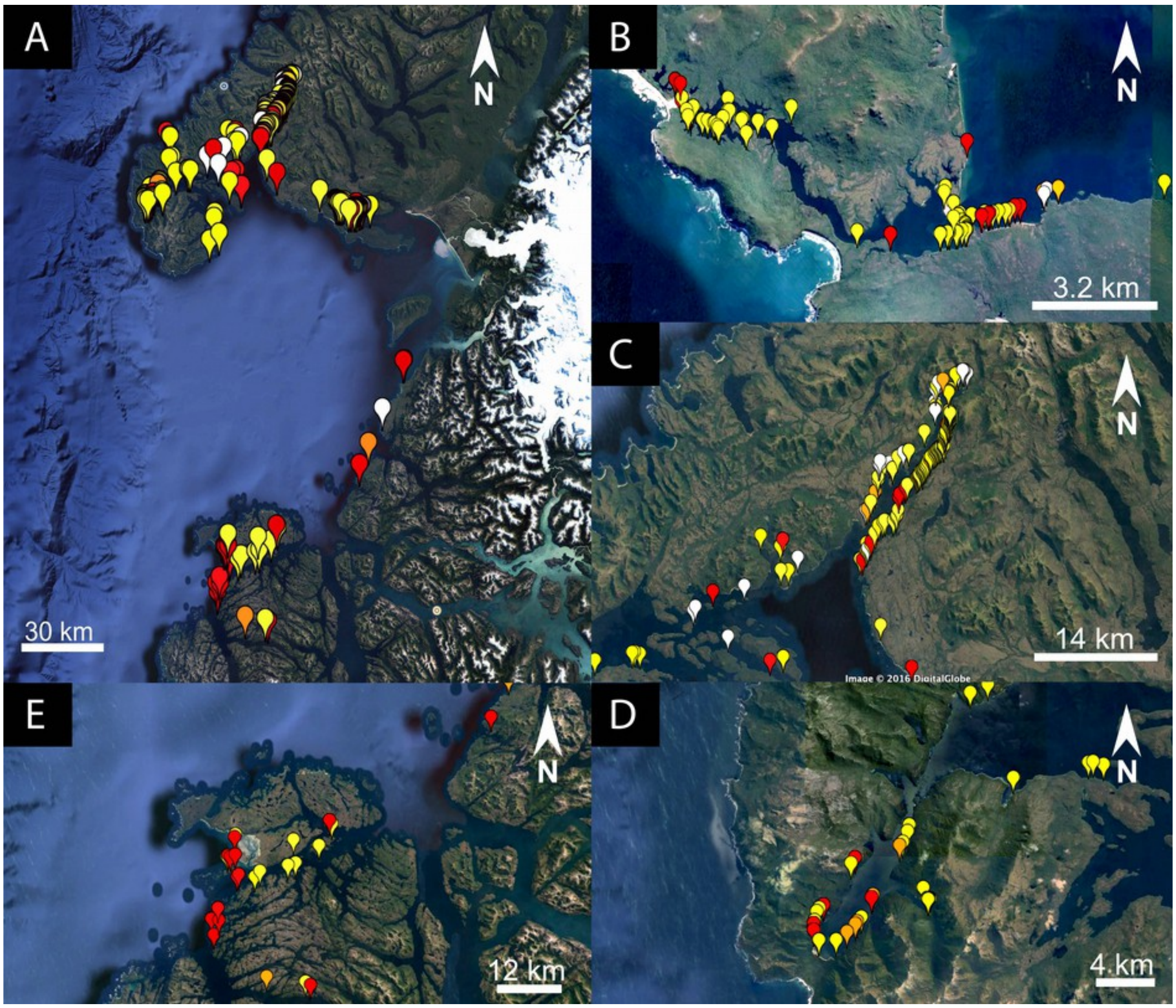

PeerJ Preprints | https://doi.org/10.7287/peerj.preprints.2707v1 | CC BY 4.0 Open Access | rec: 6 Jan 2017, publ: 6 Jan 2017

Fig. 10: Inflation of the tongue and its implication for whale carcass deposition. The greater proportion of carcasses deposited in a lateral position and to a lesser extent in the ventral-up position reflects the hydrodynamics of the body in the sea as determined by the inflation of the abdominal region (*9*) and mainly of their tongues. A) inflated tongue in a very recently dead sei whale (weeks) indicated by the arrow head. B) Close-up of the mouth with dislocate mandibles due to the previous inflation of the tongue (arrow head), which is decayed and removed by scavengers. C) Whale carcass seen from the overflight deposited in lateral position and its protuberant inflated tongue (arrow head).

Fig. 11: Graphs showing the proportion of the total classified carcasses in the biostratonomic analysis. A) Time since death, B) Time since death, combining Class 1 and 2, C) location of death, D) Anatomical positions of carcasses (lateral, ventral and dorsal-up).

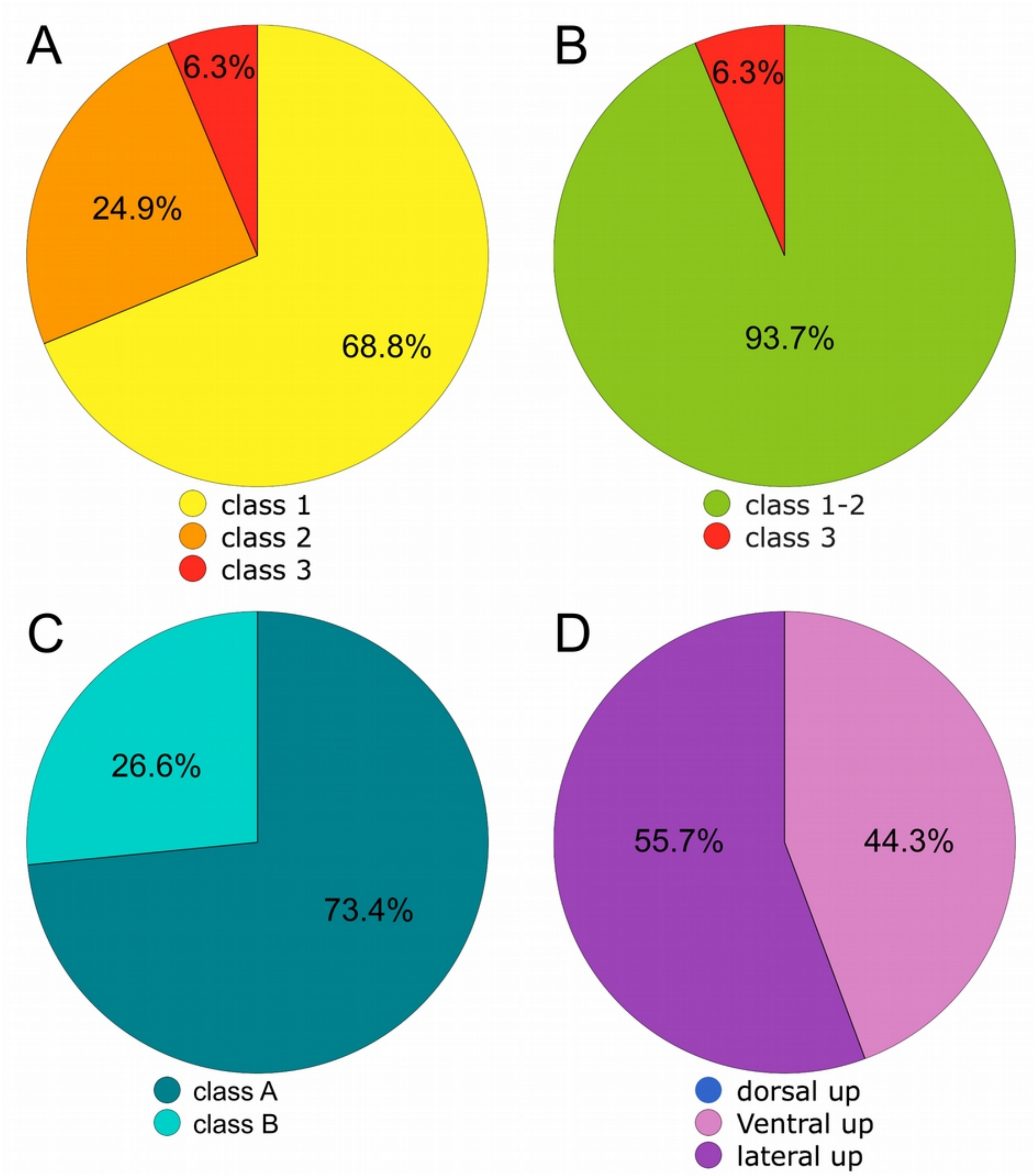

Fig. 12: Location of beached carcasses (blue) predicted by the drift model from four possible mortality locations (red stars). Mortalities during a 2-month period are simulated, from mid February to mid April 2015, with multiple carcasses (n=200) of varying drift properties released each day to predict the range of resulting carcass locations. Green vectors show time-averaged surface currents for this period (HYCOM model). Depth contours at 50 m and 100 m are indicated (GEBCO), although nearshore waters and inlets are not resolved.

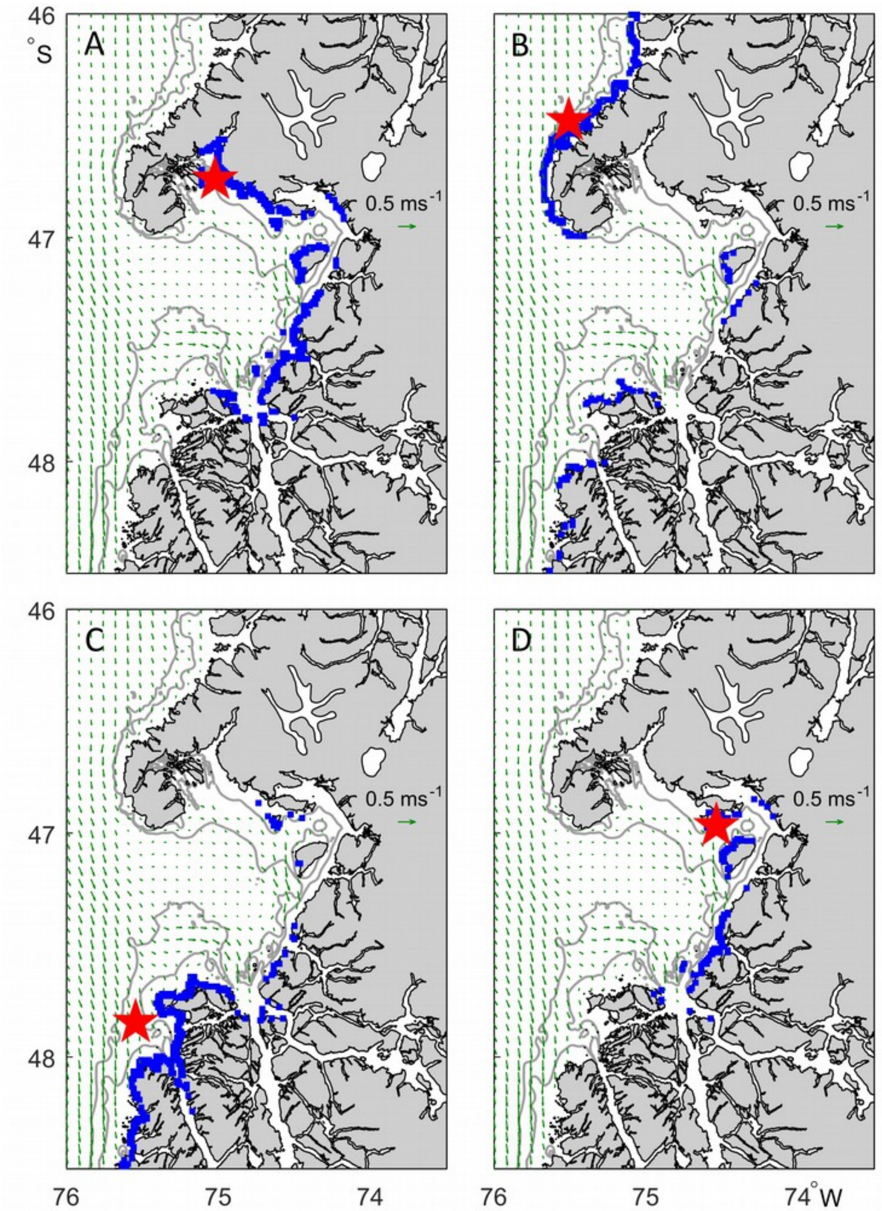

Fig. 13: Cumulative alongshore component of near-shore wind stress (red) from ECMWF ERA-Interim reanalysis winds at three latitudes, with an origin time of the vernal equinox, September 21, 2014. Gray shading shows the envelope of variability experienced during 1995−2014, with darker shading indicating one standard deviation from the mean for this period. Vertical lines show the timing of vessel (green) and aerial (blue) observations of whale carcasses.

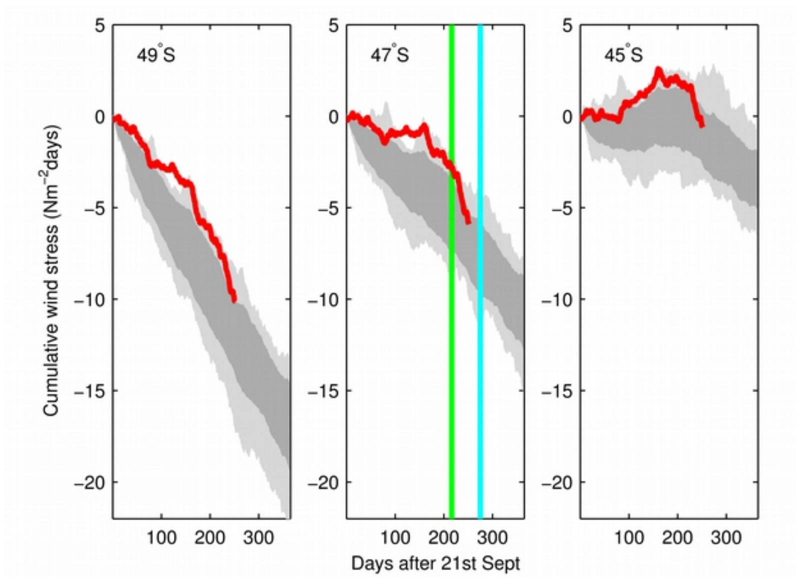

PeerJ Preprints | https://doi.org/10.7287/peerj.preprints.2707v1 | CC BY 4.0 Open Access | rec: 6 Jan 2017, publ: 6 Jan 2017

919 **Fig. 14:** Spatial distribution of PST (STX. Eq./100g tissue) as measured in mytilids and the relative abundance of *Alexandrium catenella* between 43°S and 51°S in March 2015. Insert shows the toxin level at the closest site to the Golfo de Penas, Isla Canquenes (45°43´31"S; 74°06´51"W) measured between March 2010 and March 2015. Shellfish consumption is unsafe for humans if values rise above 80μg STX. Eq./100g tissue.

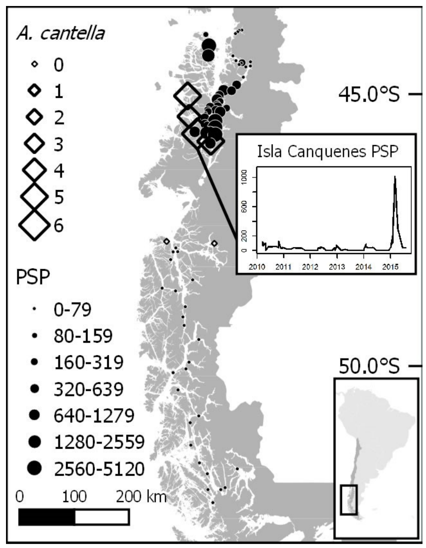

Fig. 15: Spatial distribution of PST (STX. Eq./100g tissue) as measured in mytilids between 43°S and 51°S in March 2016. In 2016, the PST levels in the Golfo Tres Montes region were not elevated. However, values four to seven times higher than usual peaks were measured in the channels of Central Patagonia. Shellfish consumption is unsafe for humans if values rise above 80µg STX. Eq./100g tissue.

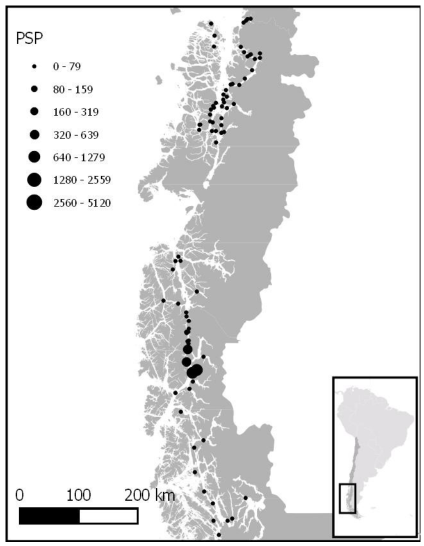

Fig. 16: Wind roses at the entrance to two inlets, Seno Newman (A) and Estero Slight (B), derived from a local high-resolution implementation of the WRF model. Spoke lengths indicate the frequency of occurrence of winds from each direction. Colors represent speed. Seno Newman has a significant up-inlet component (winds from SSW) but Estero Slight does not (winds from NNE).

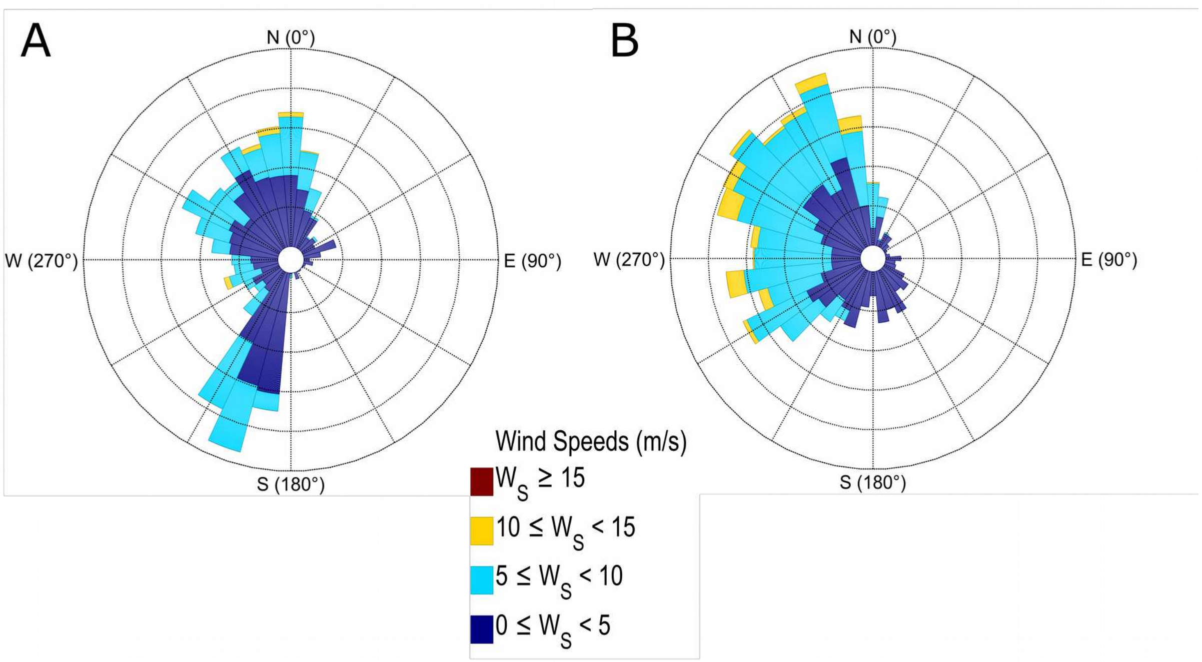

PeerJ Preprints | https://doi.org/10.7287/peerj.preprints.2707v1 | CC BY 4.0 Open Access | rec: 6 Jan 2017, publ: 6 Jan 2017

Fig. 17: Nautical maps of Escondido and Slight Inlet. A) Section of the Bahia San Quintin showing Escondido Inlet (maximum depth 15m). B) Section of Hoppner Bay showing Estero Slight (maximum depth 152m). Sources: Map nr 8820 and 8810 from armada de Chile. Newman Inlet is poorly charted with only five depths indicated along the inlet, the largest being 82m.

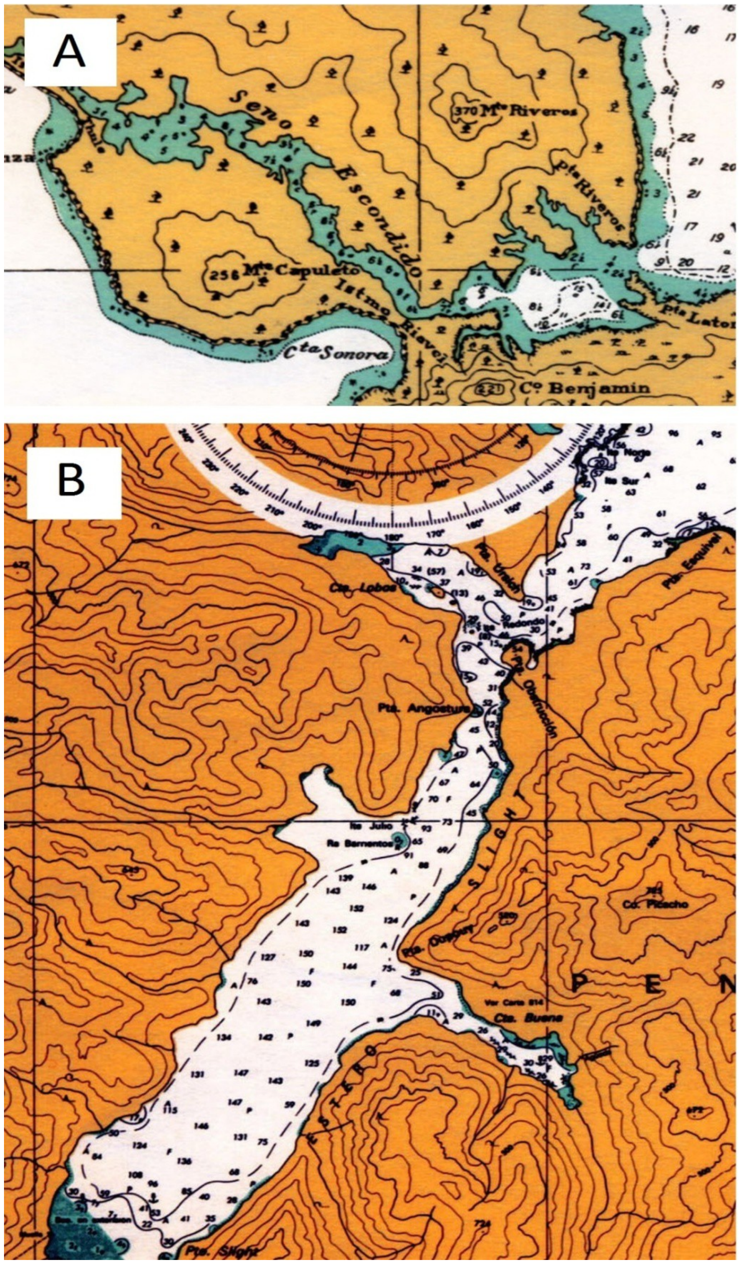

PeerJ Preprints | https://doi.org/10.7287/peerj.preprints.2707v1 | CC BY 4.0 Open Access | rec: 6 Jan 2017, publ: 6 Jan 2017

Table 1: Recorded mass mortality events of baleen whales (updated from Table 1 in Rowntree et al. (2013))

Region/site	Time span	Species	Number	Age classes	Cause of death	Source
Caleta Buena/Slight Inlet, Southern Chile	November/December 1977	rorqual	4 fresh, numerous skeletons		unknown	Pers. Comm. Salas M, 2015
Cape Cod (USA)	5 weeks (11/1987)	humpback	14		HAB (saxitoxin)	Geraci et al., 1989
Upper Gulf of California (Mexico)	? (1995)	fin, minke and bryde[1]	8		unknown	Vidal & Gallo-Reynoso, 1996
Eastern North East Pacific	throughout 1999	gray	283[2]	mostly adults	malnutrition?	Gulland et al., 2005
Eastern North East Pacific	throughout 2000	gray	368	mostly adults	malnutrition?	Gulland et al., 2005
Upper Gulf of California (Mexico)	? (2009)	unknown	10		unknown	Rowntree et al., 2013
Australia	throughout 2009	humpback	46	mostly calves and juv.	unknown	Coughran et al., 2013
Brazil	throughout 2010	humpback	96	mostly calves and juv.	unknown	Rowntree et al., 2013
Peninsula Valdés (Argentina)	2005-2011[3]	southern right	420	mostly calves	unknown (HAB-related?, starvation?, kelp gull harassment?)	D'Agostino et al., 2015; Wilson, 2015
Puerto Edén area (Chile)	March 2011	sei and/or minke	3		unknown	this paper
Estero Cono (Chile)	March 2012	sei and/or minke	15		unknown	Pers. comm. Fischer RM, 2015
Puerto Edén area (Chile)	January 2014	sei and/or minke	5		unknown	Pers. comm. Cristie C, 2015
Between 46° and 51°S, mainly Golfo de Penas (Chile)	February to early April 2015[4]	probably all sei	305	all	HAB	this paper
Alaska/British Columbia (USA/Canada)	Mai/June 2015	fin, humpback, grey	38		unknown (HAB?)	NOAA, 2015b

[1] In total, 400 cetaceans died, including 8 baleen whales
[2] 106 in Mexico during 3 months
[3] 116 died during 2012
[4] 271 died within one month

PeerJ Preprints | https://doi.org/10.7287/peerj.preprints.2707v1 | CC BY 4.0 Open Access | rec: 6 Jan 2017, publ: 6 Jan 2017

Table 2 (separate file)

Table 3 – Proportion of carcasses in each anatomical position as recorded from the overflight survey and posterior photographic analysis.

Anatomical position of Carcass	Unkown	Dorsal Up	Ventral Up	Lateral Up	Total
Count	187	0	43	54	**97**
Proportion (%)	65.84%	0	15.14%	19.01%	**100**
Proportion (%) based on classified individuals only	-	0	44%	56%	**100**

PeerJ Preprints | https://doi.org/10.7287/peerj.preprints.2707v1 | CC BY 4.0 Open Access | rec: 6 Jan 2017, publ: 6 Jan 2017

Table 4 – Minimal number of individuals (MNI) and proportion of carcasses in each of the classes of decomposition / disarticulation stages recorded at Golfo de Penas.

	Class	**MNI**	**Proportion (%)**
Classes of decomposition			
Time since death	1	141	68.78
	2	51	24.88
	3	13	6.34
	Total	**205**	**100**
Time at sea	A	147	97.35
	B	4	2.64
	Total	**151**	**100**

Table 5. Density of specimens in assemblages (specimens/km²).

	Area (km²)	**No. of specimens**	**Density (specimens/km²)**
Assemblage 1 - Jungfrauen Group	0.19	30	156
Assemblage 2 - Escondido Inlet	0.02	47	1906
Assemblage 3 - Escondido Inlet	0.01	32	1987
Assemblage 4 - Newman Inlet	0.60	149	248
Assemblage 5 - Slight Inlet	0.04	40	952
Total area of assemblages/specimens	0.87	298	341
Average	0.17	59	1050

PeerJ Preprints | https://doi.org/10.7287/peerj.preprints.2707v1 | CC BY 4.0 Open Access | rec: 6 Jan 2017, publ: 6 Jan 2017

976 **Table 6:** Comparison of the usual causes of death with the evidence encountered at Golfo the Penas (GP).

Cause of death for marine mammals	Main feature	Type of evidence (confirm-discard)	Observation at Golfo de Penas	Expected in rorqual event	Oceanographic conditions near time of death	Rorqual Species recorded	References	Oceanographic Conditions Observed at GP
Starvation by abundance surpassing carrying capacity	Thin blubber layer, or empty stomach, or numbers around 5% of population	Measurements, necropsy and population numbers nearby carrying capacity	Not likely, Sei whales are still recovering from whaling, last species to be hunted	Reported in one species	Low productivity event	Unknown. Reported in gray whales (*Eschrichthius robustus*).	Gulland et al. 2005	High productivity event
Epidemic Disease	Morbillivirus: Contagious-epidemic, emaciated, external and internal parasites, lesions and inflammatory reactions	Histology, parasitology-virology test	No signs of external or internal lesions in the whales of Estero Slight. Stomach content present. No test available.	Low numbers, young individuals.	Shift in temperature, anthropogenic contamination, mutation of virus.	Juveniles and calves fin whales, *Balaenoptera physalus*	Brongersma-Sanders 1957, Jauniaux et al. 2000, Shimizu et al 2013, Van Bressem et al. 2014, Mazzariol et al. 2016	Unknown
Military exercise with Sonar	Only confirmed in dolphins	ear damage and – or haemorrhage nearby the ears	Unknown	Unknown	No military exercises public programed, chilean law for the protection of whales	Unknown	Goldbogen et al. 2013, Nowacek et al. 2007, Southall et al. 2007	Not reported
Poisoning by toxins of Harmful Algal Bloom	Massive, multispecific, recurrent in time	HAB reported, shift in oceanographic conditions, El Niño event	Yes	Yes	High productivity event, El Niño influence	*Balaenoptera physalus, Megaptera novaeangliae, Balaenoptera acutorostrata*	Geraci et al. 1989, Fire et al. 2010, Pyenson et al. 2014, Brongersma-Sanders 1957. (Present work)	Yes, at the closest station of red tide monitoring.
Trauma: Ship collision/ entanglement	Evidence of trauma, small number (i.e. 8 deaths in 19 years in U.S.A.)	Lesions, hematoma,	No sign of internal or external lesion.	Yes (small number of individuals at a time)	Not related.	*Eubalaena glacialis*	Kraus, 1990; Moore et al. 2004, Vanderlann y Taggart, 2007.	Not related.

977

978

Table 7 – Main biostratinomic pathways and their significance in understanding the thanatocenosis.

Time since death	**Condition of the carcasses**	**Age proportions**	**Sex proportions**	**Geographic position**	**Observed**
Catastrophic – single event	Highly homogenous. Majority within one to a few classes (*42*)	Same as population rate	Same as population rate	Homogenous	Homogenous; see Tab. S2
Time averaged	Highly heterogeneous. Several classes present.	Same as proportion of annual mortality of the population.	No pattern, different from ratio of population.	Heterogeneous	Homogenous; see Tab. S2

Location of death	**Condition of the carcasses**	**Anatomic position expected**	**Anatomic position expected**	**Orientation**	**Anatomic position observed**
Authoctonous	Very well preserved, low disarticulation	Position of life: dorsal up (*5*).	Dorsal up	No trend	Dorsal up: 1.00%
Allocthonous	Disarticulation and scattering present, depending on time and distance to final deposit	Heterogeneous depending on time since death or time of drift. Majority ventral to lateral up (*5*, see Fig. S5).	Ventral up – lateral up	One main direction (current-wind) and/or two main directions (tide)	Ventral up: 20.40% Lateral Up: 78.61%